WATER RESOURCES RESEARCH, VOL. 17, NO. 4, PAGES 1191-1211, AUGUST 1981

Scale-Dependent Dispersion in a Stratified Granular Aquifer

JOHN F. PICKENS AND GERALD E. GRISAK

National Hydrology Research Institute, Inland Waters Directorate, Environment Canada, Ottawa, Ontario, Canada K1A 0E7

The magnitude of longitudinal dispersivity in a sandy stratified aquifer was investigated using laboratory column and field tracer tests. The field investigations included two-single-well injection-withdrawal tracer tests using ^{131}I and a two-well recirculating withdrawal-injection tracer test using ^{51}Cr-EDTA. The tracer movement within the aquifer was monitored in great detail with multilevel point-sampling instrumentation. A constant value for dispersivity of 0.7 cm was found to be representative (and independent of travel distance) at the scale of an individual level within the aquifer. A dispersivity of 0.035 cm was determined from laboratory column tracer tests as a representative laboratory-scale value for sand from the field site. The scale effect observed between the laboratory dispersivity and the dispersivity from individual levels in the aquifer is caused by the greater inhomogeneity of the aquifer (e.g., laminations within individual layers) and the averaging caused by the groundwater sampling system. Full-aquifer dispersivities of 3 and 9 cm obtained from the single-well tests indicate a scale effect with the value obtained being dependent mainly on the effect of transverse migration of tracer between the layers and the total injection volume. The full-aquifer dispersivity of 50 cm from the two-well test is scale-dependent, controlled by the distance between the injection and withdrawal wells (8 m) and hydraulic conductivity distribution in the aquifer. Scale-dependent full-aquifer dispersivity expressions were derived relating dispersivity to the statistical properties of a stratified geologic system where the hydraulic conductivity distribution is normal, log normal or arbitrary. In the developed expressions, dispersivity is a linear function of the mean travel distance. Proportionality constants ranged from 0.041 to 0.256 for the hydraulic conductivity distributions obtained from the field tracer tests.

INTRODUCTION

Analysis and prediction of solute transport in hydrogeologic systems generally involves the use of some form of the advection-dispersion equation. In general terms, advection describes the mean transport rate (velocity) of a solute, and hydrodynamic dispersion (molecular diffusion plus mechanical dispersion) explains the variation about the mean. If one could define exactly the three-dimensional flow pattern in the pore channels of a porous medium, then it is conceivable that the transport of all solute particles could be described by the processes of advection and molecular diffusion alone. Since it is impractical, if not impossible, to define flow at this microscopic scale, averaging of the groundwater velocity over some representative volume is necessary. This averaging introduces some uncertainty in the velocity, with the uncertainty manifest in the mechanical component of the hydrodynamic dispersion coefficient. The averaging, or the scale that one chooses to define the flow domain and obtain groundwater samples, can result in a scale dependence of the mechanical dispersion coefficient or dispersivity.

The main objectives of this paper are to develop a theoretical basis for the quantification of scale-dependent dispersion in stratified granular media and to show from detailed monitoring and analysis of several field tracer tests that longitudinal dispersivity is dependent on the scale of groundwater sampling. These objectives were accomplished by (1) developing theoretical scale-dependent full-aquifer dispersivity relationships, based on the hydraulic conductivity distribution, for solute transport in stratified media, (2) conducting laboratory tracer tests on a repacked core from the aquifer to yield laboratory-scale dispersivities, (3) conducting field tracer tests in a sandy stratified aquifer with detailed spatial and temporal sampling using multilevel groundwater point-sampling instrumentation at various distances, (4) obtaining statistical properties of the hydraulic conductivity distribution for the stratified aquifer from analysis of tracer movement at various depths and calculating the corresponding scale-dependent dispersivity expressions for the aquifer, and (5) obtaining longitudinal dispersivity values from analysis of the tracer tests at the scale of the full aquifer thickness and the individual levels within the aquifer. The practical application of the concepts discussed in this paper and the incorporation of scale-dependent dispersivity functions in a solute transport model are presented by *Pickens and Grisak* [1981].

Paper number 1W0532.
0043-1397/81/001W-0532$01.00

SCALE-DEPENDENT DISPERSION

An apparent scale effect in solute dispersion in porous media has become particularly noticeable since the early 1970's. This has been primarily due to the relatively large dispersivity values required to adequately model existing contamination zones with computer simulation techniques. Table 1 lists the values of longitudinal (and transverse) dispersivities obtained from computer modeling studies of contamination zones in granular geologic media. The longitudinal dispersivities range from 12 to 61 m, with a slight trend for larger dispersivities to be associated with larger contamination zones. These values are in marked contrast to the longitudinal dispersivities obtained from analysis of laboratory breakthrough-curve data on repacked granular materials, which are of the order of 0.01–1 cm [e.g., *Lau et al.*, 1958, 1959; *Bear*, 1961*b*; *Hoopes and Harleman*, 1967*a*; *Hartel*, 1972; *Reynolds*, 1978]. Intermediate to these two contrasts are the longitudinal dispersivities obtained from analysis of various types of field tracer tests (Table 2) which range between 0.012 and 15.2 m (with the exception of a dispersivity of 460 m reported by *Cole* [1972] from analysis of the data of *Theis* [1963]).

Most of the contamination zone studies and field tracer tests used groundwater sampling techniques which provided mixed samples from large vertical intervals. The length of the intake zone varied from several meters to several tens of meters. Groundwater sampling at these scales was likely a significant factor in the determination of the large dispersivities that were

TABLE 1. Field Dispersivity Values in Granular Material Obtained From Results of Contamination Zone Modeling

Reference	Areal (A), Cross-Sectional (C), or One-Dimensional (O)	Length of Zone, m	Longitudinal Dispersivity, m	Transverse Dispersivity, m
Pinder [1973]	A	~1,300	21.3	4.3
Robson [1974]	A	>8,000	61	n.r.
Konikow and Bredehoeft [1974]	A	~18,000	30.5	9.2
Fried [1975]	O	~800	15	1
	O	600–1,000	12	4
Konikow [1976]	A	~13,000	30.5	n.r.
Robson [1978]	C	~3,500	61	0.2
Wilson and Miller [1978]	A	~1,300	21.3	4.3

Note: n.r. means not reported.

reported in these studies. The exceptions in Tables 1 and 2 are the studies by *Sudicky and Cherry* [1979] and *Lee et al.* [1980] which used point-sampling instrumentation similar in design to that used in the tracer tests presented in this paper. The dispersivities that were obtained in these two studies and the preliminary results of the work presented in this paper [*Pickens*, 1978; *Pickens et al.*, 1978*a*, 1980] are considerably smaller than those from the other studies listed in Tables 1 and 2.

Scale dependence in field dispersion studies has been recognized by a number of investigators. *Theis* [1962, 1963] reasoned that the increased longitudinal dispersion observed in the field, as compared to the laboratory, must result from the wide distribution of permeabilities and consequently velocities found within an aquifer. *Fried* [1972] reported longitudinal dispersivities from several sites which were 0.1 to 0.6 m for the local (aquifer stratum) scale, 5 to 11 m for the global (aquifer thickness) scale, and 12.2 m for the regional (several kilometers) scale. *Fried* [1975] redefined these scales in terms of 'mean traveled distance' of the tracer or contaminant as (1) local scale, between 2 and 4 m, (2) global scale 1, between 4 and 20 m, (3) global scale 2, between 20 and 100 m, and (4) regional scale, larger than 100 m (usually several kilometers). *Fried* [1972] found no scale effect on the transverse dispersion coefficient and reasoned than its value could be obtained from laboratory results. However, *Klotz et al.* [1980] determined from a field tracer test that the width of the tracer cloud increased linearly with travel distance. Although not noted by the authors, the reported results provide direct evidence of an increase in the value of the transverse dispersion coefficient with increasing travel distance. *Oakes and Edworthy* [1977] conducted two-well pulse and radial injection experiments in a sandstone aquifer and found the dispersivity value for the fully penetrated depth to be 2–4 times the values for discrete layers.

Although the field tracer test studies of *Peaudecerf and Sauty* [1978], *Sudicky and Cherry* [1979], and *Lee et al.* [1980] have illustrated a scale effect, there is evidence given in each of these tests, which were analyzed assuming a one-dimensional flow field, to suggest that the scale effect may have been at least partially a consequence of streamline effects. In

TABLE 2. Field Dispersivity Values in Granular Materials Obtained From Results of Tracer Tests

Reference	Type of Test	Distance Between Wells, m	Slotted Length of Wells, m	Longitudinal Dispersivity, m
Theis [1963] (cited by *Cole* [1972])	natural gradient	3500	n.r.	6
		4000	n.r.	460
Mercado [1966]	single-well injection-withdrawal			
	injection-withdrawal	n.a.	34	0.09–0.15
	observation wells	≤115	12–39	0.50–1.50
Percious [1969]	single-well injection-withdrawal	n.a.	30.5	0.08–0.25
Wilson [1971] (cited by *Robson* [1974])	two-well nonrecirculating withdrawal-injection	79.2	14.6	15.2
Wilson [1971]	single-well injection-withdrawal	n.a.	15.2	0.25–0.33
Fried et al. [1972]	single-well pulse (individual layers)	n.a.	0.25 layers	0.1–0.6
Krefi et al. [1974]	two-well pulse	5–6	n.r.	D/V = 0.18
Robson [1974]	two-well recirculating withdrawal-injection	6.4	27.4	15.2
Fried [1975]	natural gradient	<12	n.r.	4.25
	radial injection	n.r.	n.r.	11.0
G. E. Grisak (unpublished data, 1977)	single-well injection-withdrawal	n.a.	1.8	0.29
Rousselot [1977]	natural gradient	≤60	n.r.	1
Peaudecerf and Sauty [1978]	uniform gradient	≤32.5	n.r.	1–2.7
Sauty [1978]	two-well pulse	9	n.r.	6.9
		6	n.r.	0.3
Sudicky and Cherry [1979]	natural gradient	≤14	point sampling	0.01–0.22
Sauty et al. [1979]	single-well injection-withdrawal			
	central well	n.a.	n.r.	1
	observation wells	≤13	n.r.	0.18 × radius
Lee et al. [1980]	natural gradient	≤6	point sampling	0.012

Note: n.r. means not reported, and n.a. means not applicable.

groundwater flow situations where the streamlines are not parallel but rather diverge or converge in some manner, analyses using a one-dimensional model may yield an apparent decrease or increase, respectively, in the interpreted value of longitudinal dispersivity. The spreading and reversal of spreading in the direction of flow results from the requirement of conservation of mass and may also be caused by porosity and moisture content variations within a porous medium. For unsaturated media, this spreading behavior has been illustrated in the experimental studies by *Merritt et al.* [1979]. The importance of streamline effects on advection and dispersion of solutes in surface waters has been noted, for example, by *Chapman* [1979] who utilized a transformed coordinate system to eliminate this 'geometrical' dispersion.

APPLICABILITY OF THE ADVECTION-DISPERSION EQUATION

The applicability of the advection-dispersion equation for describing solute transport in heterogeneous media and the nonuniqueness of the dispersivity value in specific situations have been investigated theoretically by several researchers. *Warren and Skiba* [1964] and *Mercado* [1967] showed that the dispersion coefficient or amount of spreading is a function of travel distance in stratified geologic media. *Schwartz* [1977] demonstrated, using a Monte Carlo technique, that a unique value of dispersivity may not exist for certain hypothetical geologic media. *Smith and Schwartz* [1980] used a hybrid deterministic-probabilistic approach to investigate the transport of a population of tracer particles in a hypothetical heterogeneous medium. They concluded that a constant 'dispersivity value for a geologic unit can theoretically exist if the system is long enough to provide sufficient spatial averaging' of the tracer particles in the velocity field.

Gelhar et al. [1979] used a stochastic approach to investigate the longitudinal dispersion resulting from vertical variations of hydraulic conductivity in a stratified aquifer. Their results demonstrated that for large time the longitudinal dispersivity approached a constant or asymptotic value which was dependent on the statistical properties of the medium. They found that the approach to this asymptotic value of dispersivity was slow and that non-Fickian transport could occur early in the process. They felt that some of the dependence of dispersivity on the scale of field experiments may simply reflect this early-time behavior. They further suggested that it may not be possible to determine the asymptotic dispersivity from field tests because of the large distances and travel times required. *Matheron and de Marsily* [1980] showed that solute transport in stratified media (with flow parallel to the stratification) is not, in general, correctly represented by the conventional advection-dispersion equation. For 'flow not strictly parallel to the stratification (i.e. a perpendicular flow component, however small, is added),' they suggest that Fickian behavior will take place asymptotically for large time or travel distance. They recommended that the medium be represented in fine detail in three dimensions, so that 'the appearance of asymptotic behavior will be faster and thus the dispersion equation will be valid much earlier.' The above theoretical studies have raised a number of questions regarding the use of the advection-dispersion equation with a constant dispersivity to describe solute transport in heterogeneous media over all time and distance scales. However, it has not been demonstrated that a practical alternative exists for solute transport modeling.

For solute transport to be accurately represented with the advection-dispersion equation using a constant value for the dispersion coefficient, the spatial variance of the solute distribution must increase linearly with time or mean travel distance in a one-dimensional system. Deviations from this behavior are well established in studies of solute transport in surface waters which utilize a similar advection-dispersion equation. *Chapman* [1979] states, that for solute transport in surface waters, the one-dimensional solution to the advection-dispersion equation with a constant dispersion coefficient 'provides a reasonable description of the dispersion in real three-dimensional channels after the elapse of a certain time, the convective period during which lateral mixing processes are completed.' Although the transport environments in surface and groundwater regimes are different, the existence of deviations from classical advective-dispersive transport at early times or short travel distances may be analogous.

If the spatial variance of the solute distribution increases proportional to the square of the travel distance, a direct linear dependence of the dispersion coefficient with travel distance is indicated. *Day* [1975] presented data for an extensive series of experiments in several streams and found that the variance of the solute distribution increased approximately with the square of the distance (power ranging from 1.84 to 2.13). *Day* [1975] also analyzed the tracer tests of *Godfrey and Frederick* [1970] and *Yotsukura et al.* [1970] and found similar results, with the variance varying with travel distance to the power of 1.34 to 2.87 for Godfrey and Frederick and 2.17 for Yotsukura et al. These studies were presumably all representative of the early-time 'convective period' described by *Chapman* [1979], as there was no evidence that the spreading was approaching the situation where transport could be described with a constant value for the dispersion coefficient.

In hydrogeologic systems the dispersion coefficient is usually assumed to be the product of dispersivity and the average water (or interstitial water) velocity. If the dispersion coefficient increases linearly in a constant-velocity hydrogeologic system, there is then a linear dependence of dispersivity on travel distance. Scale-dependent full-aquifer dispersivity expressions, based on a statistical description of the hydraulic conductivity distribution of a stratified aquifer, are developed in this paper illustrating a linear dispersivity–travel distance behavior.

SCALE-DEPENDENT FULL-AQUIFER DISPERSIVITY RELATIONSHIPS

A schematic diagram of a horizontally stratified aquifer with layers of hydraulic conductivity K_i and corresponding thickness b_i is shown in Figure 1. Flow is from left to right with a tracer introduced continuously as a vertical planar source at the input position. The shaded portion indicates the extent of tracer movement after a certain period of time has elapsed. Plug flow conditions for tracer movement are assumed in each layer. The sampling location has a well slotted throughout all the layers. The concentration of a groundwater sample obtained from the sampling well is dependent on the concentration, hydraulic conductivity, and thickness of the layers.

Mercado [1967] investigated the spreading pattern of injected water (containing a tracer) in a permeability stratified aquifer, similar to that shown in Figure 1, and found that an S-shaped transition zone (similar to that caused by dispersion) could result between the injected water and the aquifer water.

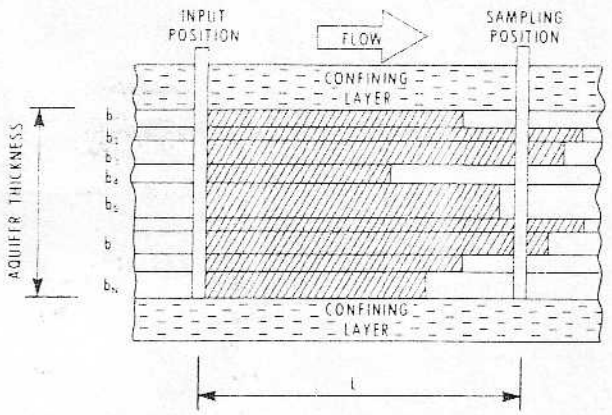

Fig. 1. Schematic cross section of tracer movement by plug flow in a horizontally stratified aquifer.

Mercado derived an expression for the width of the tracer distribution in the direction of flow, assuming groundwater is sampled over the full aquifer thickness, as

$$\sigma = (\sigma_K/\bar{K})L \tag{1}$$

where σ is the standard deviation of the tracer distribution, $\bar{K}$ and σ_K are the mean and standard deviation, respectively, of the hydraulic conductivity distribution, and L is the mean distance traveled. The assumptions used were as follows: (1) the geologic system is horizontally stratified, (2) each layer is continuous, (3) groundwater flow is horizontal, (4) hydrodynamic dispersion along the layers and between the layers is neglected since its contribution to spreading is small when compared to that due to the stratified flow, (5) the hydraulic gradient is constant and horizontal in each layer, (6) the porosity is a constant for the entire geologic system, and (7) the hydraulic conductivity or permeability distribution follows approximately a normal distribution.

From *Scheidegger* [1954] and *Day* [1956], it is noted that the dispersion coefficient D is equal to one-half of the time rate of increase of the variance of the tracer distribution (called the Einstein equation, after *Einstein* [1905]). Similarly, *Bear* [1961*a*, *b*] presented and also demonstrated experimentally that dispersivity α is a function of the variance σ^2 of the tracer distribution and the travel distance:

$$\alpha = \tfrac{1}{2}\, d\sigma^2/dx \tag{2}$$

where x is the distance coordinate. Combining equations (1) and (2) yields an expression for longitudinal dispersivity α_L in a stratified aquifer with normally distributed hydraulic conductivities as [*Pickens*, 1978; *Gelhar et al.*, 1979]

$$\alpha_L = (\sigma_K/\bar{K})^2 L \tag{3}$$

Warren and Skiba [1964] investigated miscible displacement in a hypothetical three-dimensional heteorogenous porous medium using a model based on the Monte Carlo technique. They assumed the dispersion resulted solely from the variation in permeability of the porous medium. They derived an expression for the macroscopic dispersion coefficient D for an equivalent stratified medium written

$$D = \frac{VL}{2}\,\{\tfrac{1}{4}[(8S^2 + 1)^{1/2} - 1]\} \tag{4}$$

where S^2 is the variance of the residence-time distribution, V is the interstitial flow velocity, and L is the length of the system (or mean travel distance). S^2 is defined by

$$S^2 = (\bar{K} - K_H)/K_H \tag{5}$$

for arbitrary stratification and

$$S^2 = \exp(\sigma_l^2) - 1 \tag{6}$$

for a continuous log normal permeability distribution where $\bar{K}$ and K_H are the mean and harmonic average hydraulic conductivities, respectively, and σ_l is the standard deviation of the log normal hydraulic conductivity distribution. *Warren and Cosgrove* [1964] presented a technique for determining σ_l from a plot of log permeabilities on probability paper. Assuming that the longitudinal dispersivity α_L is equal to D/V, then the resulting expression for dispersivity can be written

$$\alpha_L = \tfrac{1}{8}[(8S^2 + 1)^{1/2} - 1]L \tag{7}$$

The statistical properties of the sandy stratified aquifer investigated in this paper were determined from single-well injection-withdrawal and two-well recirculating withdrawal-injection tracer tests which were monitored in detail using multilevel point-sampling instrumentation. Equations (3) and (7) were used to obtain scale-dependent dispersivity relationships at the scale of the full aquifer thickness using these statistical properties. However, it will become evident in this paper that, at the scale of an individual level in the aquifer, the dispersivity has apparently quickly reached an asymptotic or constant value with no scale dependence observed with increasing travel distance.

TRACER TEST METHODS

Single-Well Injection-Withdrawal Tracer Test

In the single-well injection-withdrawal tracer test (hereafter called single-well test), tracer-labeled water of constant concentration is injected into a well for a certain period of time followed by pumping the same well to obtain a withdrawal-phase concentration history at the well. The flow conditions are assumed to be radially diverging and converging, respectively, to be in steady state, and to be dominant compared to the natural groundwater velocities. Dispersivity values can be obtained from analysis of breakthrough curves at observation wells or sampling points at various radial distances from the injection well during the injection phase and also from analysis of the concentration history of the injection-withdrawal well during the withdrawal phase. The single-well technique was presented initially by *Mercado* [1966] in the study of the spreading pattern of injected water bodies in a sandstone aquifer.

The unique aspects of the single-well and two-well tracer tests presented in this paper are the use of detailed point-sampling instrumentation for monitoring the tracer movement in the aquifer at many depths and distances allowing (1) evaluation of the statistical properties of the hydraulic conductivity distribution of the aquifer and calculation of scale-dependent dispersivity expressions at the scale of the full aquifer thickness and (2) evaluation of the dispersivities describing tracer migration at the scale of individual levels within the aquifer.

Hoopes and Harleman [1967*a*] presented a general equation for describing the transient concentration distribution during plane radial flow from a well as

$$\frac{\partial C}{\partial t} + V\frac{\partial C}{\partial r} = \alpha V\frac{\partial^2 C}{\partial r^2} + \frac{D^*}{r}\frac{\partial}{\partial r}\left(r\frac{\partial C}{\partial r}\right) \quad (8)$$

where C is the concentration, t is time, V is the average pore water velocity, α is the longitudinal dispersivity, r is the radial distance coordinate, and D^* is the solute molecular diffusion coefficient in the porous medium.

The longitudinal dispersivity for the full aquifer thickness can be estimated from the withdrawal-phase concentration history for the injection-withdrawal well plotted as relative concentration versus the ratio of the withdrawal (pumped) volume to the total injected volume [*Mercado*, 1966]:

$$\alpha = \frac{3U_I^{1/2}[\Delta(U_P/U_I)]^2}{32\pi^{3/2}(b\theta)^{1/2}} \quad (9)$$

where U_I is the total injected volume at the end of the injection phase, U_P is the withdrawal volume at various times during the withdrawal phase, $\Delta(U_P/U_I)$ is the dimensionless withdrawal-volume increment between the intercepts of the tangent line at $0.5C_0$ (C_0 is the input concentration) with the $C/C_0 = 0.0$ and 1.0 lines, b is the aquifer thickness, and θ is the porosity. *Gelhar and Collins* [1971] obtained a solution for the relative concentration at the injection-withdrawal well during the withdrawal phase written

$$\frac{C}{C_0} = \tfrac{1}{2}\operatorname{erfc}\left\{\left|\frac{U_P}{U_I} - 1\right|\Big/\left[\frac{16}{3}\frac{\alpha}{R}\cdot\left(2 - \left|1 - \frac{U_P}{U_I}\right|^{1/2}\left(1 - \frac{U_P}{U_I}\right)\right)\right]^{1/2}\right\} \quad (10)$$

where R is the average radial frontal position at the end of the injection phase and is defined by

$$R = (Qt/\pi b\theta)^{1/2} \quad (11)$$

The longitudinal dispersivity can also be estimated from the breakthrough curve of relative concentration C/C_0 versus time at an observation sampling well or point using the expression (adapted from *Mercado* [1966])

$$\alpha = (3r/16\pi)(\Delta t/t_{0.5})^2 \quad (12)$$

where Δt is the time increment between the intercepts of the breakthrough curve tangent line at $0.5C_0$ with the $C/C_0 = 0.0$ and 1.0 lines and $t_{0.5}$ is equal to the time at which the relative concentration C/C_0 equals 0.5 at radius r.

Analytical solutions to equation (8) at a radial distance r with a constant input concentration C_0 have been obtained by *Hoopes and Harleman* [1967*a*] and *Gelhar and Collins* [1971]. The solution by *Gelhar and Collins* [1971] offers the advantages of including the effects of finite well radius and molecular diffusion and also eliminating the initial condition limitation of the *Hoopes and Harleman* [1967*a*] solution. For injection into a stratified aquifer, the *Gelhar and Collins* [1971] solution for concentration C in layer i is written

$$\frac{C}{C_0} = \tfrac{1}{2}\operatorname{erfc}\left\{(r^2 - r_i^2)\Big/\left[16\alpha\left(\frac{\bar{r}_i^3 - r_w^3}{3} + \frac{D^*}{\alpha A_i}\frac{\bar{r}_i^4 - r_w^4}{4}\right)\right]^{1/2}\right\} \quad (13)$$

where r_w is the well radius, $\bar{r}_i$ is the average radial front position in layer i at time t, and A_i is defined by

$$A_i = (Q/b)_i/2\pi\theta \quad (14)$$

where $(Q/b)_i$ is the recharge per unit aquifer thickness in layer i. The parameter $(Q/b)_i$ is obtained from the breakthrough curve for an observation well or sampling point at a radius r and is defined by

$$(Q/b)_i = r^2\pi\theta/t_{0.5} \quad (15)$$

The average radial front position $\bar{r}_i$ in layer i at a time t is calculated from

$$\bar{r}_i = [(Q/b)_i t/\pi\theta]^{1/2} \quad (16)$$

The relationship between the molecular diffusion coefficient in a free-water system (D_0) and in a saturated porous medium (D^*) has received considerable attention in the soils and petroleum engineering literature and to a lesser extent in the hydrogeologic literature. A review of values for the ratio D^*/D_0 used by various investigators for saturated, granular, unconsolidated materials reveals a range in magnitude from the square of the porosity [*Lerman*, 1979] to a value of 0.7 [*Perkins and Johnston*, 1963]. A ratio of 0.5 has been assumed for the field and laboratory tracer tests conducted in this study.

Two-Well Recirculating Withdrawal-Injection Tracer Test

In the two-well recirculating withdrawal-injection tracer test (hereafter called the two-well test), water is withdrawn from one well and injected at an equal rate with the tracer into a second well. The flow regime is assumed to be in steady state, and the effect of natural regional flow is generally assumed to be negligible in the vicinity of the two wells. The breakthrough curve at the withdrawal well is analyzed to obtain a dispersivity value representative of solute transport at the scale of the full aquifer thickness (or screened thickness).

The steady state flow field in an aquifer from a pair of injection and withdrawal wells operating simultaneously at equal flow rates has been investigated theoretically by *DaCosta and Bennett* [1960], *Hoopes and Harleman* [1967*b*], *Grove et al.* [1970], *Webster et al.* [1970], and others. In general, the aquifer is assumed to be infinite, homogeneous, isotropic, and confined between two parallel horizontal planes. The injection and withdrawal wells are treated as a line source and line sink, respectively. Assuming that the effect of the regional flow field is negligible, the transit time for plug flow along the shortest streamline between the two wells is given by the expression [*Webster et al.*, 1970]

$$t_m = \pi\theta b d^2/3Q \quad (17)$$

where t_m is the transit time for plug flow between the two wells, θ is the porosity, b is the aquifer thickness, d is the distance between the two wells, and Q is the withdrawal-injection rate.

The dispersion of a solute in a two-well flow field has been investigated theoretically by *Hoopes and Harleman* [1967*b*], *Webster et al.* [1970], and *Grove and Beetem* [1971]. *Hoopes and Harleman* [1967*b*] developed analytical expressions in integral form for the concentration distribution in the aquifer and at the withdrawal well for a nonrecirculating well pair. They concluded that (1) dispersion and diffusion along the streamlines determine the shape of the concentration distribution within the aquifer, (2) at the pumping well, dispersion and diffusion have an important influence on the concentration history only for small concentrations ($C/C_0 < 0.1$) and for short dimensionless times ($\tau < 0.7$), (3) for $C/C_0 > 0.1$ and

$\tau > 0.7$, the concentration history at the withdrawal well is dominated by advection along the streamlines, and (4) dispersion and diffusion across the streamlines retard the rate of increase of concentration at any point within the aquifer, but this effect is small in the region of the two wells. The dimensionless time is defined by

$$\tau = 2Qt/(\pi b\theta d^2) \tag{18}$$

where t is time.

Webster et al. [1970] and *Grove and Beetem* [1971] adopted an approach of dividing the flow field between the injection and withdrawal wells into crescents. These crescents were assumed to represent columns of known length. They applied the *Brenner* [1962] solution to the one-dimensional advection-dispersion equation to calculate breakthrough curves for the outlet of each crescent. By summing the contribution from each crescent, a composite breakthrough curve for the withdrawal well was calculated. If the two-well system was recirculating, then the calculation procedure accounted for tracer that was being withdrawn from the withdrawal well and reintroduced at the injection well. The tracer addition at the injection well can be either continuous or a pulse (in time). The parameters used in the calculation procedure are the number of crescents, withdrawal-injection rate, distance between the two wells, dispersivity, porosity, and the time of tracer addition. In general, dispersivity is the unknown and is varied until the calculated breakthrough curve closely matches the field-measured breakthrough curve. The principal difference between the presentations by *Webster et al.* [1970] and *Grove and Beetem* [1971] is that the latter have adopted a more general technique employing a computer code. The code is included in the report by *Grove* [1971].

Laboratory Column Tracer Test

The equation describing the transient concentration distribution for a nonreactive solute during steady one-dimensional flow in a homogeneous column of porous media can be written

$$\frac{\partial C}{\partial t} = D\frac{\partial^2 C}{\partial x^2} - V\frac{\partial C}{\partial x} \tag{19}$$

where C is the concentration, t is time, and D and V are the hydrodynamic dispersion coefficient and average pore water velocity, respectively, in the direction of flow x. In this system, the streamlines are assumed to be parallel and in the direction of flow. For a continuous input concentration C_0 for $t > 0$, the one-term analytical solution obtained by *Rifai et al.* [1956] for (19) can be expressed in terms of pore volumes as (adapted from *Brigham* [1974])

$$\frac{C}{C_0} = \tfrac{1}{2}\left[\operatorname{erfc}\left(\frac{1-U}{2(UD/VL^*)^{1/2}}\right)\right] \tag{20}$$

where U is the number of effluent pore volumes and L^* is the column length. Brigham recommended plotting effluent relative concentration versus $[(U-1)/U^{1/2}]$ on linear probability paper. If the data fit a straight line, then the use of a 'diffusion' equation model approach was validated, and the dispersion coefficient could be calculated from the slope of the line. Anomalies in the data, resulting from dead-end pores, channeling, or improper column packing could be identified, in some cases, using this graphical method. Defining $\gamma = [(U-1)/U^{1/2}]$, the dispersion coefficient can be calculated from the expression

$$D = (VL^*/8)(\gamma_{0.84} - \gamma_{0.16})^2 \tag{21}$$

where $\gamma_{0.84}$ and $\gamma_{0.16}$ correspond to relative concentrations C/C_0 of 0.84 and 0.16, respectively.

The hydrodynamic dispersion coefficient is assumed to be the sum of (1) a mechanical dispersion part which is a linear function of the average pore water velocity and (2) a molecular diffusion part. This is expressed

$$D = \alpha_L V + D^* \tag{22}$$

where α_L is the longitudinal dispersivity and D^* is the solute molecular diffusion coefficient in the porous medium. The dispersivity value is evaluated by rearranging (22) to yield

$$\alpha_L = (D - D^*)/V \tag{23}$$

FIELD STUDY SITE

Hydrogeology

A detailed account of the physical hydrogeology of the groundwater flow system at the study site, located at the Chalk River Nuclear Laboratories, has been given by *Parsons* [1960], and recent work has been summarized by *Cherry et al.* [1975] and *Jackson and Inch* [1980]. A stratigraphic cross section through the flow system and field site is shown in Figure 2. The sand aquifers are glaciofluvial in origin. Laminations of the order of 0.1–0.5 cm and textural variations over depths of the order of several centimeters to tens of centimeters have been observed from vertical borehole cores. The tracer tests were conducted in the unit denoted as the middle-sand aquifer. The middle-sand aquifer is approximately 8.2 m in thickness, located between 2.0 and 10.2 m depth, and is confined below by a silty-clay unit about 1 m in thickness and above by about 17 cm of silt and clay. Under natural conditions, flow is horizontal in the sand aquifers and toward the lake. Aquifer response to pumping a well in the middle-sand aquifer has shown that the middle-sand and lower-sand are hydraulically isolated from each other at the tracer test site by the silty-clay unit. The upper-sand aquifer exhibits minor head changes due to pumping or injection in the middle-sand aquifer.

The hydraulic conductivity of the middle-sand aquifer, determined during this study by short-term and long-term aquifer response tests to a fully penetrated pumping well and by slug tests on piezometers (slotted length of 0.6 m) is in the range of 2×10^{-3} to 2×10^{-2} cm/s. Full-aquifer hydraulic conductivities for the middle-sand aquifer were also obtained from the single-well and two-well tracer tests. For the single-well test denoted SW1 using an injection rate of 0.886 l/s, field measurements of the change in hydraulic head (from natural flow conditions) versus radial distance from the injection well for 23 piezometers at distances of 1.0–14.9 m were fit to the regression equation

$$h = 0.512 - 0.275 \log_{10} r \tag{24}$$

where h is the increase in hydraulic head (m) and r is the corresponding radial distance (m). Using this equation in conjunction with the Thiem flow equation [*Kruseman and de Ridder*, 1970, p. 47] yields a full-aquifer hydraulic conductivity of 1.4×10^{-2} cm/s. A full-aquifer hydraulic conductivity of 1.0×10^{-2} cm/s was evaluated from the two-well test using the

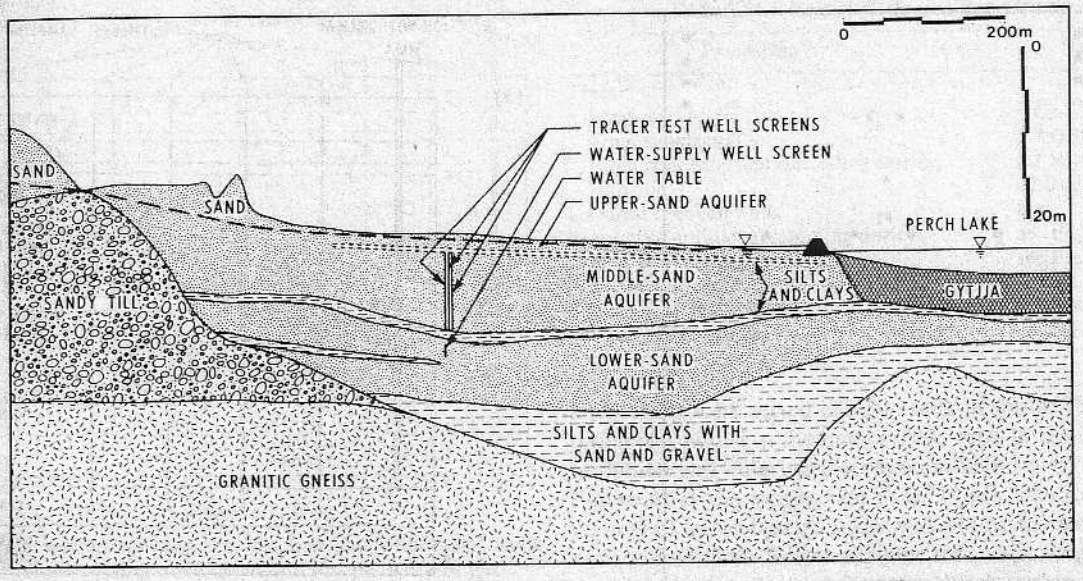

Fig. 2. Stratigraphic cross section through the field study area showing location of tracer test wells.

equation given by *De Wiest* [1965, p. 249] for the steady state drawdown at the withdrawal well of a two-well withdrawal-injection flow field. Since well losses were difficult to quantify and not deducted from the measured drawdown of 0.43 m in the withdrawal well, this hydraulic conductivity is likely an underestimate.

Grain size determinations were conducted on sediment core samples from 16 depths throughout the middle-sand aquifer. The samples were from cores obtained from boreholes drilled for installation of the injection and withdrawal wells for the tracer tests. The range of grain size distributions from the samples is shown in Figure 3. These sands are classed as very fine to medium grained (Wentworth classification) and well sorted. The mean grain size ranged from 0.12 to 0.21 mm with a mean and standard deviation of 0.16 and 0.003 mm, respectively. The uniformity coefficient ranged from 1.6 to 4.4 with a mean and standard deviation of 2.3 and 0.8, respectively.

Parsons [1960] determined porosities in the range of 0.33–0.43 for 120 sediment samples that he classified as fine sand (65–100% of the particles by weight finer than 0.2 mm and 0–10% finer than 0.06 mm) taken from the study area. A porosity of 0.38 has been chosen as representative for the middle-sand aquifer for the present study.

Instrumentation

There is an extensive piezometer and well network at the study site and throughout the hydrologic basin. The instrumentation for conducting the field tracer tests included piezometers, wells, and multilevel sampling devices (Figure 4). The piezometers used for monitoring piezometric heads in the three aquifers during the tracer test were constructed of 2.5 cm diameter polyvinyl chloride (PVC) pipe with 0.6 m length slotted tips wrapped with fiberglass cloth. The water supply well and the injection and withdrawal wells were constructed of 10.4 cm diameter PVC pipe with manufactured No. 4 slot screens. The water supply well has a screened interval of 1.5 m located in the lower-sand aquifer. The injection and withdrawal wells were screened over approximately the full extent of the middle-sand aquifer. The piezometers and wells were installed through casing driven by wash boring and by cable-tool rig, respectively.

Tracer movement within the aquifer was monitored by obtaining groundwater samples from multiple depths at various areal locations using the multilevel point-sampling devices (Figure 5) developed by *Pickens et al.* [1978*b*]. The device consists of a bundle of 0.3 cm diameter polypropylene tubes contained inside a PVC pipe with each tube protruding through the wall of the pipe at a different elevation where it serves as a point water sampler. The tip of each tube is encased in fine-meshed stainless steel screening (intake area about 1 cm^2). The multilevel sampling devices were installed through casing driven by wash boring. Groundwater samples are obtained by vacuum pumping of the polypropylene tubes.

Cross sections of the study site showing the instrumentation for the single-well tests (denoted SW1 and SW2) and the two-well test are shown in Figures 6 and 7, respectively. The sampling points were spaced closely in the vertical direction in the middle-sand aquifer to allow a very detailed assessment of the

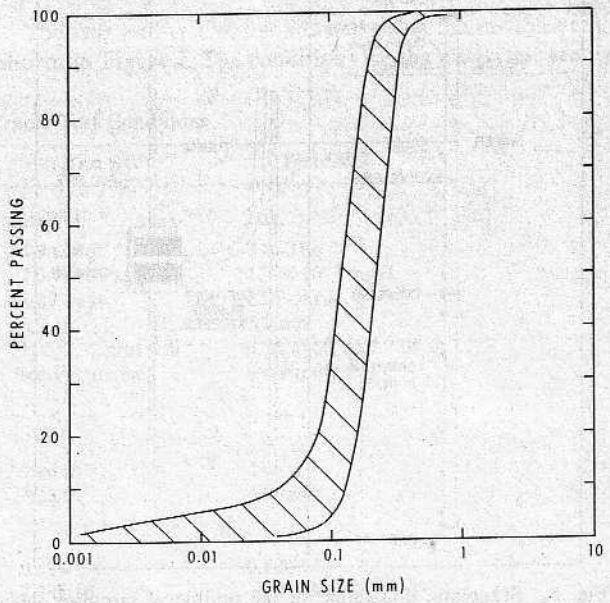

Fig. 3. Envelope of grain size distribution curves from samples taken from 16 depths within the middle-sand aquifer.

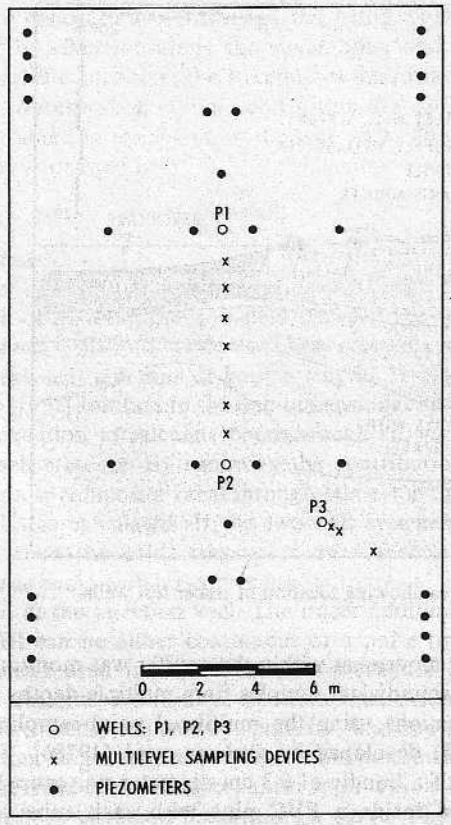

Fig. 4. Layout of the instrumentation location for the field tracer tests.

relative hydraulic conductivity distribution (stratification). Sampling points were also located above and below the middle-sand aquifer in order to assess the ability of the silt and clay layers to confine the transport of the tracer-labeled water to the middle-sand aquifer.

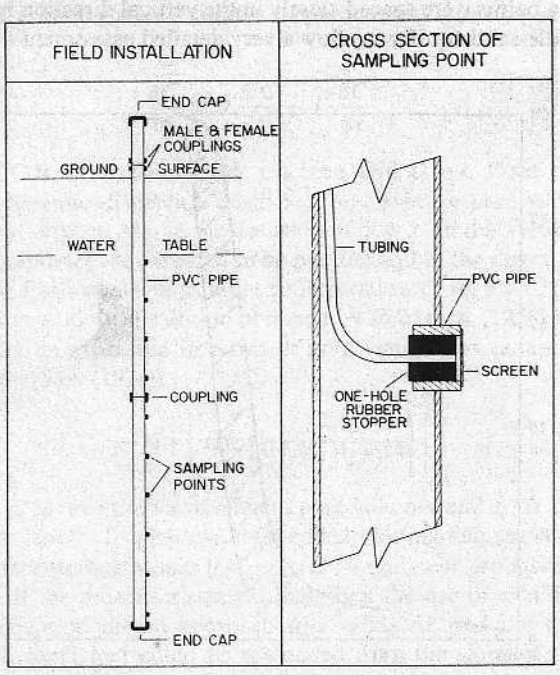

Fig. 5. Schematic illustration of the multilevel sampling device showing a field installation and a cross section of a sampling point [after *Pickens et al.*, 1978*b*].

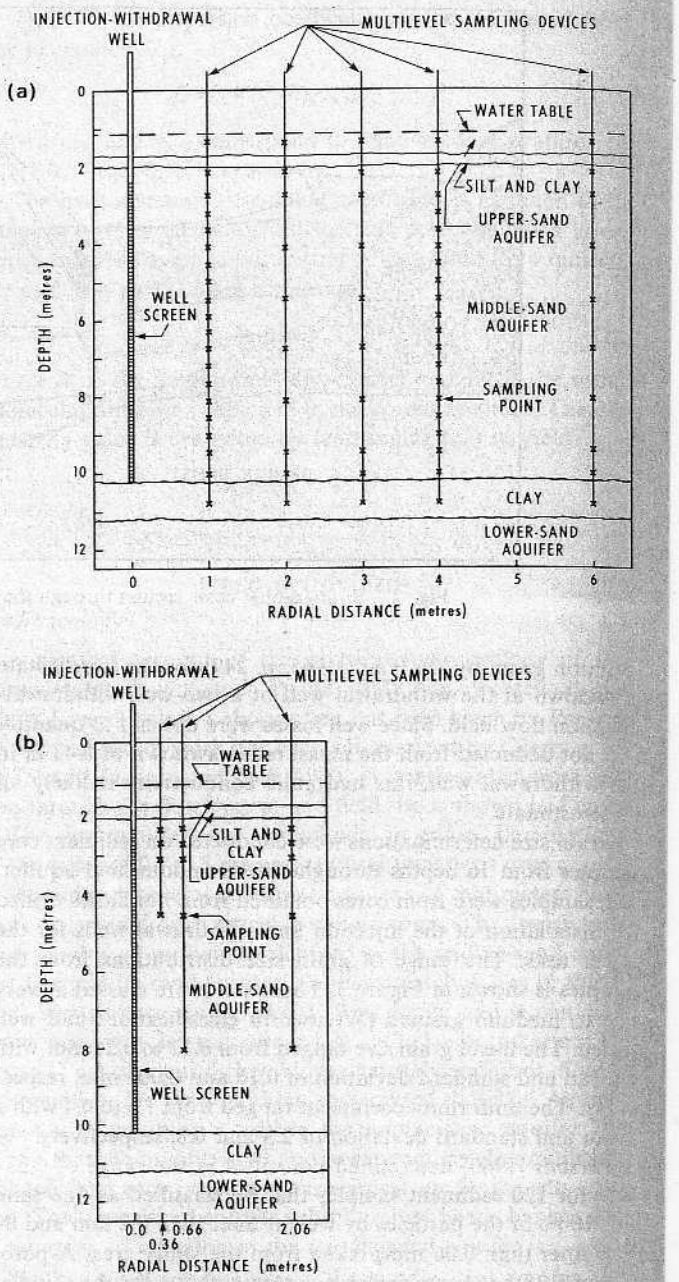

Fig. 6. Cross section showing the injection-withdrawal well and the point-sampling instrumentation for single-well tests (*a*) SW1 and (*b*) SW2.

EXPERIMENTAL PROCEDURES

Single-Well Injection-Withdrawal Tracer Tests

The single-well tests SW1 and SW2 were conducted using the instrumentation shown in Figures 6*a* and 6*b*, respectively. The test conditions are listed in Table 3. A well in the lower-sand aquifer was used for water supply (Figure 2). Water was recharged to the middle-sand aquifer at the injection rate for 1 day prior to commencing tracer addition to ensure steady state flow conditions. The piezometer network (Figure 4) at the study site was monitored to establish the hydraulic head distribution during the tests.

Test SW1. Approximately 1.9 GBq of ^{131}I and 5 mg of NaI carrier were mixed in a 13.6-l tank of water. This tracer solution was added at the rate of 0.083 ml/s to the injection water which was entering the injection-withdrawal well P1

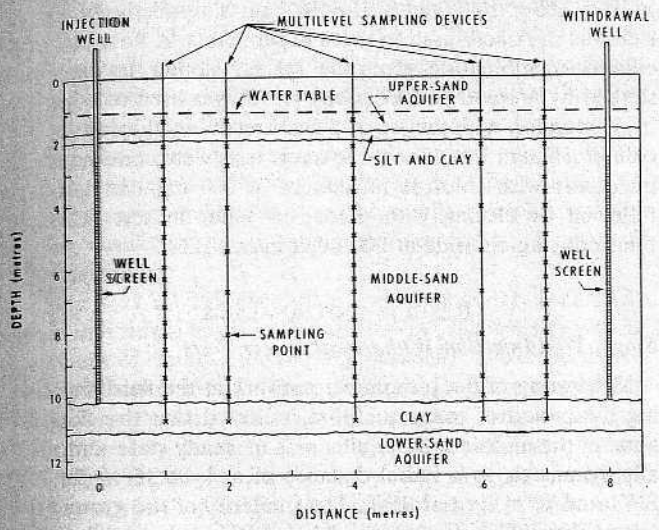

Fig. 7. Cross section showing the injection and withdrawal wells and the point-sampling instrumentation for the two-well test.

(see Figure 4) at the steady rate of 0.886 l/s. The total injection volume of tracer-labeled water was 95.6 m^3 injected over a period of 1.25 days. Water samples for monitoring tracer concentration were obtained from three levels within the injection-withdrawal well and from the total of 70 sampling points on the multilevel sampling devices located at the radial distances of 1, 2, 3, 4, and 6 m. A volume of about 100 ml of fluid was removed from each sampling tube prior to taking a 15-ml sample for analysis of tracer concentrations.

At the end of the tracer injection phase, water was pumped from the injection-withdrawal well at the rate of 0.886 l/s for 2.0 days (equivalent to 1.6 injection volumes). Water samples were obtained from the well discharge line for analysis of tracer concentration.

Ten-milliliter volumes of the samples obtained during the monitoring of the tracer test were analyzed for ^{131}I radioactivity using a gamma counter (Packard) with a 76-mm NaI (T1) well crystal. All radioactivities of the water samples were corrected for radioactive decay to the time at which the tracer test was started. They are reported as relative concentrations in comparison to the average input concentration of the tracer-labeled water during the injection phase.

Test SW2. Approximately 3.0 GBq of ^{131}I and 5 mg of NaI carrier were mixed in a 50-l tank of water. This tracer solution was added at the rate of 0.133 ml/s to the injection water which was entering the injection-withdrawal well P3 (see Figure 4) at the steady rate of 0.719 l/s. The total injection volume of tracer-labeled water was 244 m^3 injected over a period of 3.93 days. Water samples for monitoring tracer concentration were obtained from two levels within the injection well and from the total of 14 sampling points on the multilevel sampling devices located at the radial distances of 0.36, 0.66, and 2.06 m. A volume of water approximately twice the volume in each multilevel sampling tube was withdrawn and discarded prior to obtaining a 10-ml water sample for analysis of tracer concentrations. At the end of the tracer injection phase, water was pumped from the injection-withdrawal well at the rate of 0.606 l/s for 16.9 days (equivalent to 3.6 injection volumes) with water sampling from the well discharge line for analysis of tracer concentration. Five-milliliter volumes of the samples obtained during the monitoring of the tracer test were analyzed for ^{131}I radioactivity.

The reactive tracer ^{85}Sr was also included in the injection water for test SW2 to provide field estimates of the distribution coefficients for ^{85}Sr by comparing its transport rate to that of ^{131}I. The studies of the adsorptive properties of the aquifer are given by *Pickens et al.* [1981].

TABLE 4. Two-Well Tracer Test Conditions

Parameter	Value
Tracer	
Species	^{51}Cr-EDTA
Total radioactivity	3.7 GBq
Input concentration (including carrier)	4.1×10^{-6} mg/l
Half-life	27.8 days
Distance between wells	8 m
Position of multilevel sampling devices	see Figure 7
Depths of sampling points	see Figure 7
Withdrawal-injection rate	0.449 l/s
Duration of tracer addition	3.22 days
Duration of tracer test	15 days

Two-Well Recirculating Withdrawal-Injection Tracer Test

The two-well test was conducted using the instrumentation shown in Figure 7. The conditions for the tracer test are listed

TABLE 3. Single-Well Tracer Test Conditions

Parameter	Test SW1	Test SW2
Tracer		
Species	^{131}I	^{131}I
Total radioactivity	1.9 GBq	3.0 GBq
Input concentration (including carrier)	2.7×10^{-4} mg/l	1.9×10^{-5} mg/l
Half-life	8.07 days	8.07 days
Well radius	5.7 cm	5.7 cm
Radial position of multilevel sampling device	1, 2, 3, 4, and 6 m	0.36, 0.66, and 2.06 m
Depth of sampling points	see Figure 6*a*	see Figure 6*b*
Injection Phase		
Rate	0.886 l/s	0.719 l/s
Duration (from start of tracer addition)	1.25 days	3.93 days
Total injected volume	95.6 m^3	244 m^3
Average radial front position at end of injection phase	3.13 m	4.99 m
Withdrawal Phase		
Rate	0.886 l/s	0.606 l/s
Duration (from end of tracer addition)	2.0 days	16.9 days
Total withdrawal volume	153 m^3	886 m^3

TABLE 5. Laboratory Column Tracer Test Conditions

Parameter	Value
Tracer	chloride
Column length	30 cm
Column diameter	4.45 cm
Mean grain size	0.20 mm
Uniformity coefficient	2.3
Porosity	0.36
Flow rate	
Test R1	5.12×10^{-3} ml/s
Test R2	1.40×10^{-2} ml/s
Test R3	7.75×10^{-2} ml/s
Average velocity	
Test R1	9.26×10^{-4} cm/s
Test R2	2.53×10^{-3} cm/s
Test R3	8.60×10^{-3} cm/s

in Table 4. The two-well withdrawal-injection (wells P1 and P2 in Figure 4) flow regime was operated at the rate of 0.449 l/s for several days prior to the beginning of tracer addition to ensure steady state flow conditions. The piezometer network was monitored to establish the hydraulic head distribution during the test. Approximately 3.7 GBq of the tracer ^{51}Cr-EDTA with 0.5 mg of stable Cr were mixed in a 22.7-l tank of water. This tracer solution was added for 3.22 days at the rate of 0.083 ml/s to the injection water which was entering the injection well at the steady rate of 0.449 l/s. The tracer test continued for a total duration of 15 days. Water samples were obtained from the discharge line from the withdrawal well, from two levels within the injection well, and from the multilevel sampling devices located between the two wells. A volume of about 100 ml of fluid was removed from each sampling tube prior to taking a 15-ml sample for analysis of tracer concentrations. Ten-milliliter volumes of the water samples obtained during monitoring the tracer test were analyzed using a well-type gamma counter.

Laboratory Column Tracer Tests

Three laboratory column tracer tests were conducted on a repacked column of sand from a core obtained from the depth of 8.1–8.5 m at the field site. The vertically mounted column apparatus consisted of methyl methacrylate tubing with (from bottom to top) an inlet tube through a one-hole rubber stopper, a layer of No. 40 mesh stainless steel screening, a layer of No. 100 mesh stainless steel screening, the repacked sand, a layer of No. 100 mesh and No. 40 mesh stainless steel screening, and a one-hole rubber stopper with an outlet tube. The layers of wire mesh aided the radial spread of the fluid at the inlet and outlet ends of the column and also prevented the loss of fine material from within the column. The air-dried sand was put in the column by a funnel with a long extension to prevent free fall of the sand. The base of the column was tapped gently (with minimal vibration) after each 1-cm depth increment. This procedure for packing the column was adopted in order to minimize radial segregation of the sand within the column. The tracer solution was introduced at the lower end of the vertically mounted column with a tubing pump connected to a constant-head (Mariott) reservoir. All column tracer tests were conducted at about 23°C.

The significant parameters, textural characteristics, and conditions for the column tracer tests are listed in Table 5. Three experiments designated R1, R2, and R3 were conducted corresponding to average pore water velocities of 9.26 $\times 10^{-4}$, 2.53×10^{-3}, and 8.60×10^{-3} cm/s, respectively. Chloride was the tracer used in these experiments. A flow cell and chloride combination electrode system similar to that described by *Mansell and Elseftawy* [1972] was used to continuously monitor, with the aid of a chart recorder, chloride in the column effluent line. The three tracer tests were conducted sequentially with chloride introduced at 200 mg/l in test R1, followed by eluting with deionized water in test R2, and reintroducing chloride at 200 mg/l in test R3.

RESULTS AND ANALYSIS

Single-Well Injection-Withdrawal Tracer Tests

Monitoring of the piezometer network at the field site during the period of tracer addition indicated that the flow regime in the middle-sand aquifer was in steady state and radially symmetric to a radial distance of at least 15 m for test SW1 and 10 m for test SW2. The similarity of the groundwater quality of the lower-sand aquifer (water supply) and middle-sand aquifer groundwaters [*Pickens et al.*, 1981] and the small quantity of tracers added (see Table 3) ensured that the groundwater flow regime was not affected by contrasting fluid densities.

Test SW1. The relative concentration history in the injection-withdrawal well was obtained as the average from water samples from the two sampling levels within the well during the injection phase. The tracer concentrations of the water samples taken from the two levels within the well were within about 2%, indicating good mixing of the input tracer solution and the injection water. The measured input concentration from samples taken at 14 separate times varied from 95% to 103.5% of the average concentration during the 1.25 days of tracer injection.

The monitoring results of the multilevel sampling devices showed that the tracer moved at significantly different rates at different levels (layers) in the aquifer. Tracer was not detected in the shallowest or the deepest sampling points (see Figure 6*a*), providing evidence of the effectiveness and continuity of the confining layers.

Longitudinal dispersivity values for the individual levels were obtained using equation (12) by analysis of the breakthrough data (Figure 8) provided by the sampling points on the multilevel sampling devices. Dispersivity values were in the range of 0.2–9.0 cm (Table 6) from the 29 breakthrough curves. This range in individual-level dispersivities is partially the result of the few data points available to define some of the breakthrough curves and partially the result of vertical migration of tracer. The value of 9 cm was obtained for the sampling point at 8.11 m depth and 3.0 m radial distance with breakthrough data which exhibited a noncharacteristic shape with a very gradual linear increase in concentration with time after initial breakthrough (perhaps caused by a defective sampling point). Neglecting this value, the dispersivity range for test SW1 is 0.2–3.5 cm with a mean value of 0.7 cm. However, there are only three dispersivities that are more than a factor of 3 different than the mean value.

Breakthrough curves for each of the sampling points were calculated using equation (13) with the parameter values listed in Tables 3 and 6 and using an estimated diffusion coefficient in saturated porous media (at 8°C) for iodide of 6.7×10^{-6} cm^2/s. The field-measured breakthrough data and the calcutated (analytical solution) results for the sampling points compare closely as shown in Figure 8, with only a few dis-

crepancies in the later portions of the breakthrough curves. The fitting of the analytical solution to the field-measured breakthrough curves was controlled essentially by the values of the dispersivity and the recharge per unit aquifer thickness at each individual level. The contribution of molecular diffusion to the calculated breakthrough curves was negligible since the molecular diffusion coefficient was more than 2 orders of magnitude smaller than the smallest mechanical dispersion coefficient within the maximum radial distance of tracer sampling.

There was no evidence of a scale-dependent dispersivity within individual levels in the aquifer (i.e., dispersivity was independent of distance to sampling position). The dispersivities obtained from analysis of the point-sampling data suggest that a relatively constant value has been reached for each level in the aquifer (see Table 6). The relatively constant dispersivity at the individual levels can be interpreted as representative of the 'asymptotic' value (in the terminology of *Gelhar et al.* [1979] and *Matheron and de Marsily* [1980]). This asymptotic dispersivity applies only at the scale of individual levels within the aquifer with groundwater sampling using the point-sampling instrumentation.

A full-aquifer dispersivity was obtained from analysis of the withdrawal-phase concentration history of the injection-withdrawal well. The field concentration data versus the ratio of the withdrawal phase pumped volume to the total injected volume are shown in Figure 9*a*. Planimetering the area under the concentration history indicates approximately total tracer recovery during the withdrawal phase. The dimensionless withdrawal-volume increment $\Delta(U_p/U_t)$ corresponding to the intercepts of the tangent line at 0.5 C_o with the $C/C_o = 0.0$ and 1.0 lines was 0.565. The full-aquifer dispersivity is 3 cm, estimated using equation (9). The calculated concentration history obtained using equation (10) compares closely with the field data using a dispersivity and an average radial front position in the aquifer at the end of the injection phase of 3 cm and 313 cm, respectively. This full-aquifer dispersivity from test SW1 is a factor of 4.3 larger than the mean dispersivity obtained for the individual levels (0.7 cm).

Scale-dependent dispersivity relationships for the full-aquifer thickness require a detailed knowledge of the hydraulic conductivity distribution. In order to obtain the hydraulic conductivity distribution, the aquifer was divided for analysis purposes into horizontal layers b_i corresponding to each sampling point or level i (b_i is the sum of the vertical half distance to the two adjacent sampling points). The recharge per unit aquifer thickness $(Q/b)_i$ for each layer was calculated using equation (15) with the times $t_{0.5}$ to reach relative concentration $C/C_o = 0.5$ obtained from the breakthrough curves (Figure 8). Using equation (24) for hydraulic head and the Thiem equation in conjunction with the values of $(Q/b)_i$ for the multilevel sampling device located 1 m from the injection well, the hydraulic conductivity K_i for each layer was calculated. A hydraulic conductivity (K_R) relative to the layer with the largest K_i was then calculated for each of the layers. The sampling point depths with corresponding b_i, $t_{0.5}$, $(Q/b)_i$, K_i, and K_R are listed in Table 6. An illustration of the geology with the sampling-point depth locations and the relative hydraulic conductivity distribution is shown in Figure 10*a*. The sum of the product of $(Q/b)_i$ and b_i for all the layers is 0.770 l/s, which compares closely with the actual measured injection rate of 0.886 l/s.

In order to evaluate the scale-dependent dispersivity relationships at the full-aquifer scale, the aquifer stratification was characterized statistically from the relative hydraulic conductivity distribution (Table 6 and Figure 10*a*). The arithmetic average, harmonic average, and standard deviation of the relative hydraulic conductivity distribution are 0.538, 0.401, and 0.272, respectively. The relative hydraulic conductivity data were arranged in ascending order and were plotted versus percentage cumulative aquifer thickness (Figure 11*a*). The natural logarithms of the relative hydraulic conductivity data were also plotted versus percentage cumulative aquifer thickness (Figure 11*b*). The data plotted in Figures 11*a* and 11*b* can in both cases be fit approximately with straight lines. This suggests that the relative hydraulic conductivity distribution can be roughly approximated by either a normal or a log normal distribution. The standard deviation of the log normal distribution evaluated from Figure 11*b* is 0.69, and the variance of the residence-time distribution calculated using equation (5) is 0.342 for arbitrary stratification and using equation (6) is 0.610 for a continuous log normal

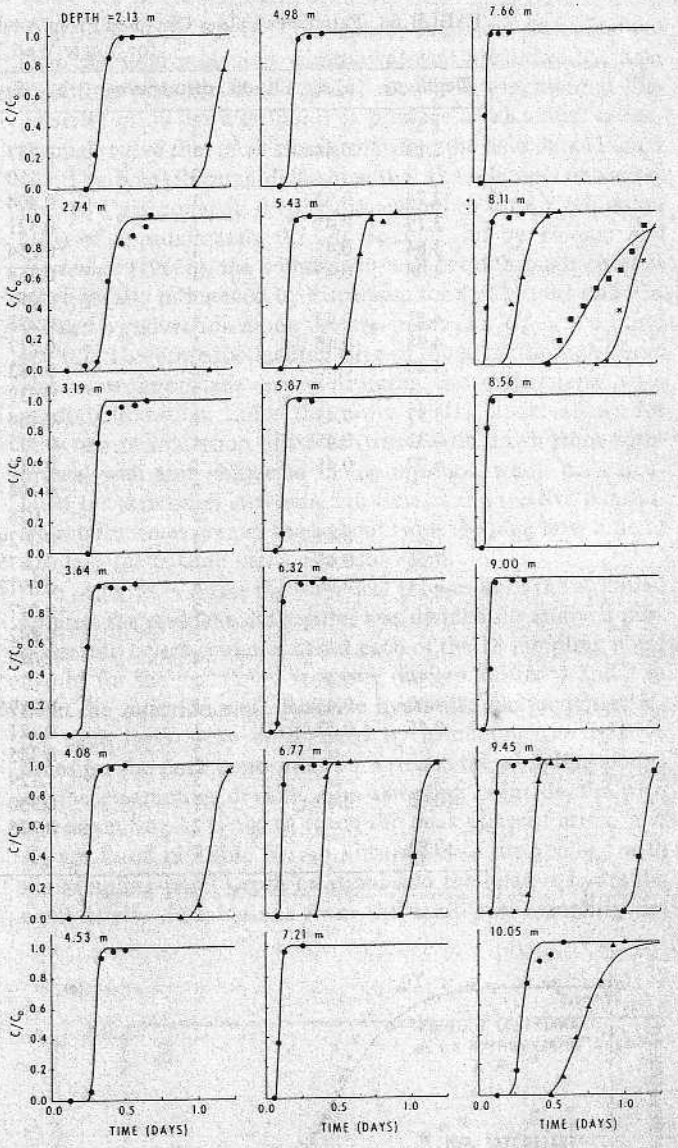

Fig. 8. Comparison of measured breakthrough curves at distances of 1 m (circles), 2 m (triangles), 3 m (squares), and 4 m (crosses) with *Gelhar and Collins* [1971] analytical solution (solid lines) for single-well test SW1. Parameter values are listed in Table 6.

TABLE 6. Parameter Values Obtained From Analysis of Breakthrough Curves From Sampling Points for Single-Well Tracer Test SW1

Depth, m	b_i, m	Radial distance, m	$t_{0.5}$, days	$(Q/b)_i$, m²/day	K_i, 10^{-2} cm/s	K_R	α, cm
1.37		1					
2.13	0.44	1	0.367	3.26	0.503	0.216	0.5
		2	1.150	4.15			0.3
2.74	0.53	1	0.404	2.95	0.457	0.196	0.6
3.19	0.45	1	0.321	3.72	0.575	0.247	0.2
3.64	0.45	1	0.254	4.70	0.726	0.312	0.5
4.08	0.45	1	0.268	4.45	0.688	0.296	0.5
		2	1.092	4.37			0.3
4.53	0.45	1	0.298	4.01	0.620	0.266	0.2
4.98	0.45	1	0.217	5.51	0.852	0.365	0.5
5.43	0.45	1	0.183	6.51	1.01	0.433	0.5
		2	0.639	7.47			0.5
5.87	0.45	1	0.144	8.30	1.28	0.550	0.5
6.32	0.45	1	0.113	10.61	1.64	0.701	0.5
6.77	0.45	1	0.116	10.27	1.59	0.683	0.3
		2	0.394	12.13			0.3
		3	1.038	10.36			0.3
7.21	0.45	1	0.0929	12.85	1.99	0.853	0.9
7.66	0.45	1	0.0875	13.64	2.11	0.905	0.5
8.11	0.45	1	0.0917	13.02	2.01	0.864	1.5
		2	0.317	15.08			3.5
		3	0.842	12.77			9.0
		4	1.083	17.63			1.5
8.56	0.45	1	0.0792	15.08	2.33	1.000	0.5
9.00	0.45	1	0.0896	13.33	2.06	0.884	0.5
9.45	0.53	1	0.121	9.88	1.53	0.655	0.3
		2	0.385	12.39			0.5
		3	1.129	9.52			0.3
10.05	0.40	1	0.300	3.98	0.615	0.264	0.7
		2	0.725	6.59			3.0
10.82		1					

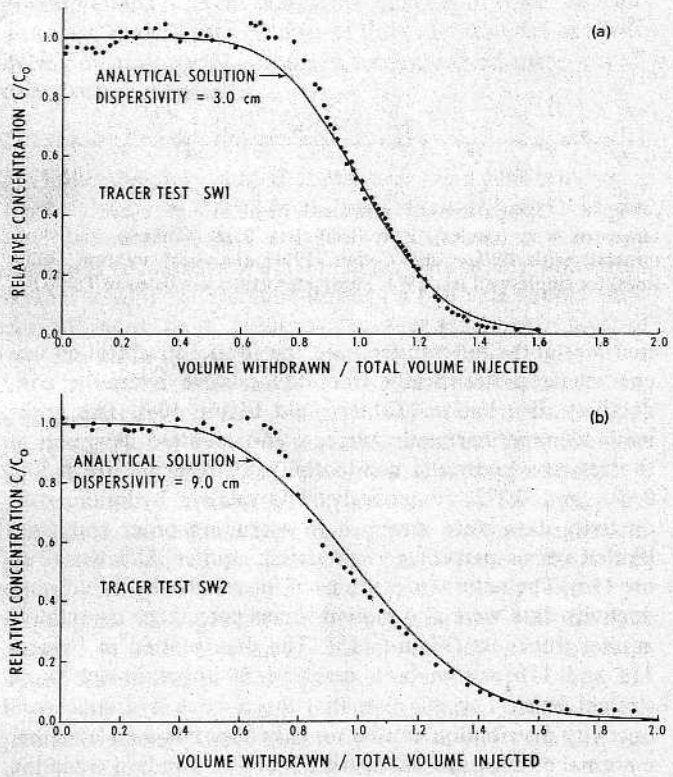

Fig. 9. Comparison of measured (circles) concentration history of the injection-withdrawal well during the withdrawal phase with the *Gelhar and Collins* [1971] analytical solution (solid line) for single-well tests (*a*) SW1 and (*b*) SW2.

hydraulic conductivity distribution. The stratification parameters are summarized in Table 7.

Scale-dependent dispersivity expressions (summarized in Table 8) were obtained using equation (3) assuming a normal hydraulic conductivity distribution and equation (7) assuming either an arbitrary or a log normal distribution. The scale-dependent dispersivity functions express dispersivity as a linear function of mean travel distance with proportionality constants of 0.256, 0.178, and 0.117 assuming normal, log normal, and arbitrary hydraulic conductivity distributions, respectively.

Test SW2. Single-well test SW2 provided dispersivities for individual levels within the aquifer and investigated the effect of a larger total injection volume on the full-aquifer dispersivity. The tracer concentrations of the water samples taken from two levels within the injection-withdrawal well during the injection phase were within about 2%. The measured input concentrations from samples taken at 19 separate times varied from 95% to 105% of the average concentration during the 3.93 days of tracer injection. The measured breakthrough data obtained for the sampling points are shown in Figure 12. The parameter values obtained from quantitative analysis of the 14 breakthrough curves are summarized in Table 9. The breakthrough curves calculated using the analytical solution (equation (13)) compare closely to the field-measured breakthrough data, as shown in Figure 12. Longitudinal dispersivities for the individual levels are in the range of 0.4–1.5 cm with a mean value of 0.8 cm. As with test SW1, there was no evidence of scale dependence at the scale of individual levels within the aquifer (Table 9). The asymptotic dis-

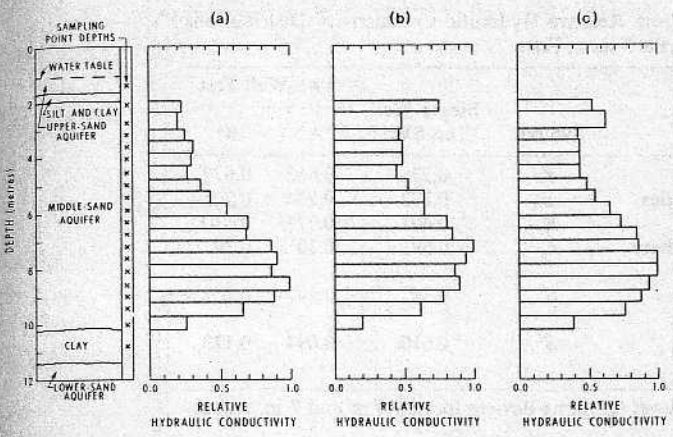

Fig. 10. Relative hydraulic conductivity distributions in middle-sand aquifer determined from monitoring tracer movement in (*a*) the single-well test SW1 and (*b*) and (*c*) the two-well test using the multilevel sampling devices at 4 m and 7 m, respectively, from the injection well.

persivity value at individual levels appears to have been reached prior to the closest sampling point position.

A full-aquifer dispersivity was obtained from analysis of the withdrawal-phase concentration history of the injection-withdrawal well (Figure 9*b*). Planimetering the area under the concentration history indicates approximately total tracer recovery. The dimensionless withdrawal-volume increment $\Delta(U_P/U_I)$ from Figure 9*b* was 0.775. The calculated concentration history obtained using equation (10) compares closely to the field data using a dispersivity (estimated using equation (9)) and an average radial front position in the aquifer at the end of the injection phase of 9 cm and 499 cm, respectively. It can be readily seen that a larger total injection volume results in a larger or scale-dependent full-aquifer dispersivity; that is, the full-aquifer dispersivity from test SW2 is a factor of 3 larger than that obtained from test SW1. The scale-dependent nature of dispersivity at the full-aquifer scale is also particularly evident by comparison to the relatively constant (asymptotic) value of 0.7 cm obtained for the individual levels.

Two-Well Recirculating Withdrawal-Injection Tracer Test

The relative concentration history in the injection well was obtained as the average from water samples from the two sampling levels within the well. The tracer concentrations of the water samples taken from the two levels within the injection well were within 10%. The measured input concentrations from samples taken at seven separate times during the 3.22 days of tracer addition to the injection water varied from 87% to 115% of the average concentration.

The results of monitoring the multilevel sampling devices showed that the tracer moved at significantly different rates at different levels in the aquifer. Breakthrough curves for the first 9 days of the tracer test for the multilevel sampling device located 4 m from the injection well, for example, are shown in Figure 13. The monitoring results obtained from all of the multilevel sampling devices indicated that the relative tracer movement was fairly consistent at any particular depth and hence that the aquifer could be considered areally homogeneous between the two wells. Tracer was not detected in the shallowest or the deepest sampling points, providing further evidence of the continuity of the confining layers of the aquifer.

A dispersivity for the full aquifer thickness was obtained from the field-measured withdrawal-well breakthrough data by fitting with the *Grove* [1971] model. A longitudinal dispersivity of 50 cm was found to produce a calculated breakthrough curve that most closely matched the field data (Figure 14). The breakthrough data show that the relative concentration C/C_o is equal to 0.1 for dimensionless time τ (equation (18)) of approximately 0.7. As pointed out by *Hoopes and Harleman* [1967*b*], the withdrawal-well breakthrough curve is more greatly influenced by dispersion for $C/C_o < 0.1$ and $\tau < 0.7$ and by advection along the streamlines for $C/C_o > 0.1$ and $\tau > 0.7$. Therefore the leading edge of the breakthrough curve was most important in determining the dispersivity with model calibration. Since the *Grove* [1971] model allows for only one recirculation of tracer (tracer withdrawn from withdrawal well and reinjected in the injection well), the calculated breakthrough curve underestimates the relative concentration for times greater than about twice the plug flow time of 5.4 days (calculated using equation (17)).

In order to evaluate the statistical properties of the stratified aquifer, the middle-sand aquifer was divided for analysis purposes into layers centered about each of the 18 sampling point depths for the multilevel sampling devices located 4 and 7 m from the injection well. Relative hydraulic conductivities K_R for each layer were determined by estimating the relative times for the peak concentration to reach the sampling points on these sampling devices. The sampling point depths with corresponding b_i, times to reach the peak concentration, and K_R are listed in Table 10. An illustration of the geology with the sampling-point depth locations and the relative hydraulic conductivity distributions from the multilevel sampling de-

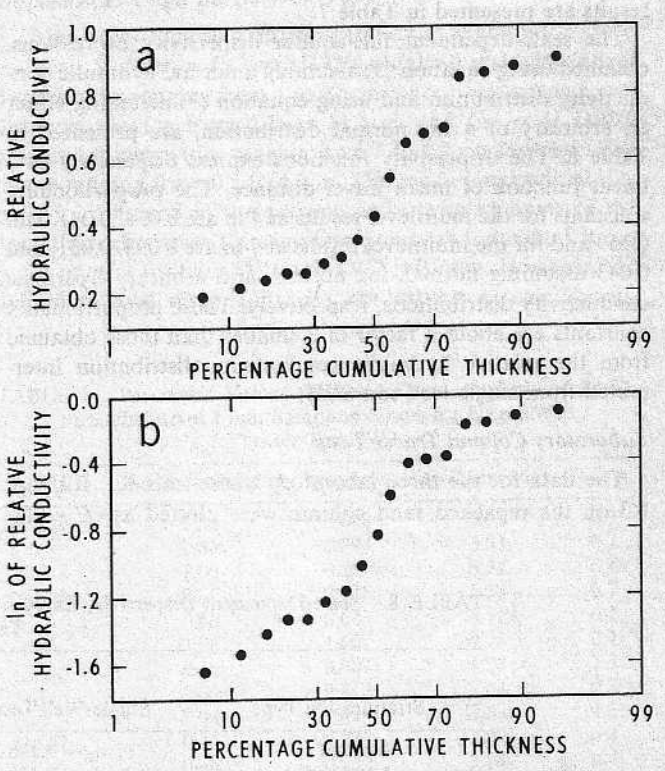

Fig. 11. Plots of (*a*) relative hydraulic conductivity and (*b*) natural logarithm of relative hydraulic conductivity versus percentage cumulative thickness of aquifer obtained from multilevel sampling device results of single-well test SW1.

TABLE 7. Stratification Parameters Evaluated From Relative Hydraulic Conductivity Distributions Obtained From the Tracer Tests

Parameter	Symbol	Single-Well Test SW1	Two-Well Test A*	Two-Well Test B*
Arithmetic average relative hydraulic conductivity	$\bar{K}$	0.538	0.662	0.672
Standard deviation of relative hydraulic conductivities	σ_K	0.272	0.204	0.205
Harmonic average relative hydraulic conductivity	K_H	0.401	0.577	0.610
Standard deviation of log normal hydraulic conductivity distribution	σ_l	0.69	0.30	0.34
Variance of residence-time distribution for arbitrary stratification	S^2	0.342	0.147	0.102
Variance of residence-time distribution for log normal stratification	S^2	0.610	0.094	0.123

* Results for A and B were obtained from multilevel sampling devices located 4 m and 7 m, respectively, from the injection well.

vices located 4 and 7 m from the injection well are shown in Figures 10*b* and 10*c*, respectively.

The aquifer stratification was characterized statistically from the relative hydraulic conductivity distributions. The relative hydraulic conductivity data were arranged in ascending order and plotted as relative hydraulic conductivity versus percentage cumulative aquifer thickness (Figures 15*a* and 16*a*) and as natural logarithms of relative hydraulic conductivity versus percentage cumulative aquifer thickness (Figures 15*b* and 16*b*). The data on these plots suggest that, for this test as well as test SW1, the relative hydraulic conductivity distribution can be roughly approximated by either a normal or log normal distribution. The arithmetic average, harmonic average, and standard deviation of the relative hydraulic conductivity distribution, the standard deviation of the log normal distribution, and the variances of the residence-time distribution for the two multilevel sampling device results are presented in Table 7.

The scale-dependent full-aquifer dispersivity expressions, obtained using equation (3) assuming a normal hydraulic conductivity distribution and using equation (7) assuming either an arbitrary or a log normal distribution, are presented in Table 8. The dispersivity functions express dispersivity as a linear function of mean travel distance. The proportionality constants for the multilevel results at 4 m are 0.095, 0.041, and 0.059 and for the multilevel results at 7 m are 0.093, 0.051, and 0.043 assuming normal, log normal, and arbitrary hydraulic conductivity distributions, respectively. These proportionality constants are about a factor of 3 smaller than those obtained from the relative hydraulic conductivity distribution interpreted from single-well test SW1.

Laboratory Column Tracer Tests

The data for the three laboratory tracer tests R1, R2, and R3 on the repacked sand column were plotted as $(U - 1)/U^{1/2}$ versus effluent relative concentration on probability paper as shown in Figure 17. The data were analyzed to obtain values of the hydrodynamic dispersion coefficient using equation (21). A value of the molecular diffusion coefficient in a free-water system at 25°C of 2.03×10^{-5} cm^2/s [*Lerman*, 1979] was assumed for the chloride ion, and the corresponding molecular diffusion coefficient in porous media was estimated to be 1.02×10^{-5} cm^2/s. The calculated hydrodynamic dispersion coefficients and corresponding dispersivities (calculated using equation (23)) for tracer tests R1, R2, and R3 are 4.05×10^{-5} cm^2/s and 0.033 cm, 8.65×10^{-5} cm^2/s and 0.030 cm, and 3.76×10^{-4} cm^2/s and 0.043 cm, respectively.

For the repacked column, the ratios of column length to diameter and column diameter to particle (mean) diameter were 6.7 and 202, respectively. These ratios were favorable in reducing the wall effect [*Hiby*, 1962; *Schwartz and Smith*, 1953]. The end-cap effect [*James and Rubin*, 1972] was considered negligible because of the length of the column in comparison to the length of the end cap. The density and viscosity difference resulting from the addition of 200 mg/l chloride was insufficient to cause unstable flow.

The average longitudinal dispersivity from the three laboratory tracer tests on the repacked column of sand from the aquifer is 0.035 cm. This value compares closely with the average value of 0.030 cm (range from 0.016 to 0.061 cm) obtained by *Reynolds* [1978] for 29 laboratory tracer tests using three laboratory columns with sand from a nearby field site.

Klotz et al. [1980] reported results from an extensive series of laboratory column tracer tests and showed that the magnitude of dispersivity measured in laboratory columns depends mainly on the effective grain size and the uniformity coefficient. From grain size analyses on samples from 16 depths within the aquifer, narrow ranges of mean grain size (0.12 and 0.21 mm) and uniformity coefficient (1.6 to 4.4) were obtained. By comparison to the graphical results of the effect of

TABLE 8. Scale-Dependent Dispersivity Expressions Obtained From Stratification Results for Tracer Tests

Stratification Type	Single-Well Test SW1	Two-Well Test A*	Two-Well Test B*
Normal	$\alpha_L = 0.256\,L$	$\alpha_L = 0.095\,L$	$\alpha_L = 0.093\,L$
Log normal	$\alpha_L = 0.178\,L$	$\alpha_L = 0.041\,L$	$\alpha_L = 0.051\,L$
Arbitrary	$\alpha_L = 0.117\,L$	$\alpha_L = 0.059\,L$	$\alpha_L = 0.043\,L$

* Results for A and B were obtained from multilevel sampling devices located 4 m and 7 m, respectively, from the injection well.

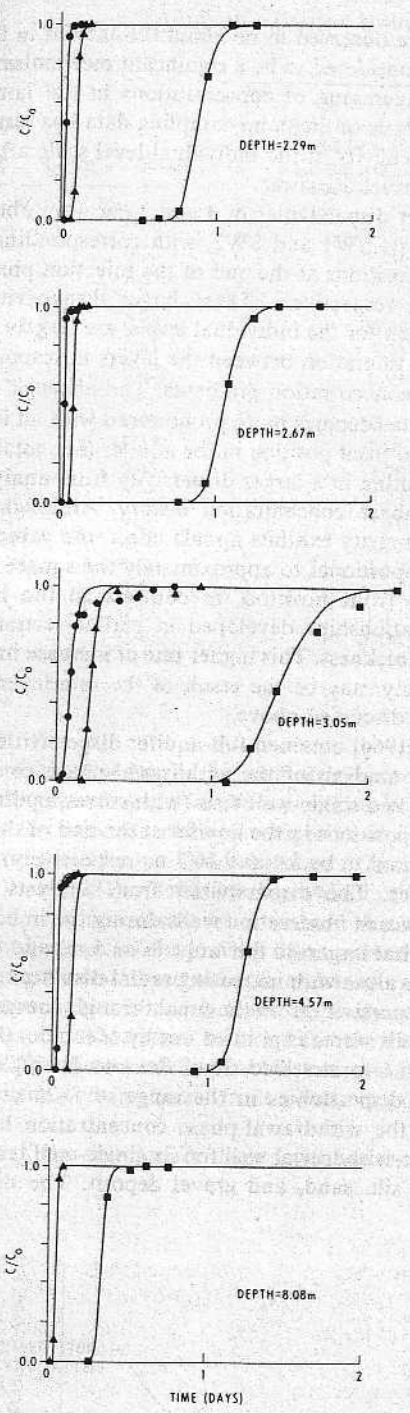

Fig. 12. Comparison of measured breakthrough curves at distances of 0.36 m (circles), 0.66 m (triangles), and 2.06 m (squares), with *Gelhar and Collins* [1971] analytical solution (solid lines) for single-well test SW2 [after *Pickens et al.*, 1981]. Parameter values are listed in Table 9.

grain size and uniformity coefficient presented by Klotz et al., it is estimated that the magnitude of laboratory-measured dispersivity obtained from samples from the aquifer would vary by less than a factor of 3. Because of this small expected variation and the close comparison to the dispersivities of *Reynolds* [1978], the average dispersivity of 0.035 cm is considered a representative laboratory-scale value for sand taken from the middle-sand aquifer.

DISCUSSION

Groundwater Sampling

Withdrawing a groundwater sample from a well, a piezometer, or a sampling point on a multilevel sampling device results in some mixing or averaging with a corresponding effect on the measured tracer concentration. For example, water samples that were obtained for analysis of tracer concentration during single-well test SW1 and the two-well test were from a thin, approximately spherical shell at a radius of about 4 cm from the sampling point intake. Therefore the sampling instrumentation causes some 'averaging' which in turn causes the measured breakthrough curves to be somewhat more spread out. This type of spreading is a function of both the sampling scale and the volume of sample withdrawn and is unavoidable in any tracer test or contamination zone monitoring where groundwater samples are removed from the geologic system. Nevertheless, the amount of flow disturbance and spreading caused by the multilevel sampling devices is much less than would result from using piezometers or wells for groundwater sampling. The spreading effect resulting from groundwater sampling from fully penetrating wells in a stratified aquifer, as compared to sampling the individual aquifer layers, has been demonstrated qualitatively by *Grisak et al.* [1979]. This effect has also been shown experimentally by *Pickens and Grisak* [1979] for a tracer test in a heterogeneous sand and gravel deposit with groundwater samples taken with both fully penetrating screened wells and multilevel point-sampling devices. As the spreading effect caused by the monitoring system increases, the dispersivity obtained from analysis of concentration profile or breakthrough curve data will also likely increase.

Dispersivities From Single-Well Tests

Using point-sampling instrumentation in sandy unconfined aquifers, *Sudicky and Cherry* [1979] obtained scale-dependent dispersivities ranging from 1 to 22 cm for corresponding travel distances ranging from 0.75 to 11.5 m, and *Lee et al.* [1980] obtained dispersivities ranging from 5 to 1.2 cm for travel distances ranging from 0.5 to 4.3 m. The mean longitudinal dispersivity obtained in the present study from analyses of the breakthrough curves for sampling points at individual levels in the aquifer for tests SW1 and SW2 is 0.7 cm. However, the individual-level dispersivity did not exhibit a scale depen-

TABLE 9. Parameter Values Obtained From Analysis of Breakthrough Curves From Sampling Points for Single-Well Tracer Test SW2

Depth, m	Radial distance, m	$t_{0.5}$, days	$(Q/b)_i$, m²/day	α, cm
2.29	0.36	0.028	5.53	0.7
	0.66	0.094	5.53	0.7
	2.06	0.88	5.74	0.7
2.67	0.36	0.028	5.53	0.7
	0.66	0.085	6.12	0.7
	2.06	1.06	4.78	0.7
3.05	0.36	0.087	1.78	1.5
	0.66	0.213	2.44	0.7
	2.06	1.43	3.54	1.5
4.57	0.36	0.038	4.07	0.4
	0.66	0.132	3.94	0.4
	2.06	1.22	4.15	0.4
8.08	0.66	0.053	9.81	0.7
	2.06	0.34	14.90	0.7

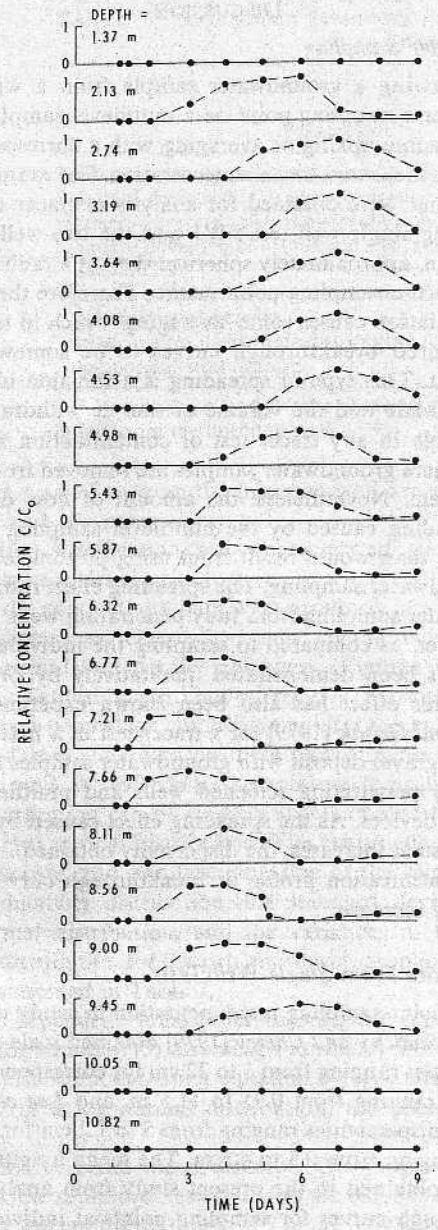

Fig. 13. Field-measured breakthrough curves (circles) for the multi-level sampling device located 4 m from the injection well for the two-well test.

dence for the various travel distances to sampling points which ranged from 0.36 to 4 m (see Tables 6 and 9).

One explanation for not observing a scale effect for dispersivity at the individual levels may be that the asymptotic dispersivity (in the terminology of *Gelhar et al.* [1979] and *Matheron and de Marsily* [1980]) has been reached at a travel distance less than 0.36 m, which is the nearest sampling position. As suggested by *Matheron and de Marsily* [1980], representing the aquifer at smaller scales (individual levels or layers) allows a much quicker appearance of the asymptotic or constant dispersivity behavior. The approach to an asymptotic dispersivity is clearly dependent both on the porous media characteristics (e.g., small-scale laminations and larger-scale aquifer layers) and on the scale of groundwater sampling. As mentioned above, the zone of influence for the point samples was approximately 4 cm radius, while laminations in the aquifer layers were observed to be about 0.1–0.5 cm in thickness. Diffusion is considered to be a significant mechanism in causing vertical averaging of concentrations in the laminations. Thus the analysis of the point-sampling data has resulted in a constant dispersivity at the individual-level scale after a relatively short travel distance.

Full-aquifer dispersivities of 3 and 9 cm were obtained for single-well tests SW1 and SW2, with corresponding average radial front positions at the end of the injection phase of 313 and 499 cm, respectively. These larger dispersivities, compared to 0.7 cm for the individual levels, are largely the result of transverse migration between the layers in response to hydraulic and concentration gradients. The effect of migration between layers becomes more pronounced with an increase in average radial front position in the aquifer (i.e., total injection volume) resulting in a larger dispersivity from analysis of the withdrawal-phase concentration history. Although the full-aquifer dispersivity exhibits a scale effect, the value obtained increases proportional to approximately the square of the average radial front position, in contrast to the linear dispersivity relationships developed in earlier sections for the full-aquifer thickness. This higher rate of increase in full-aquifer dispersivity may be the result of the interlayer transport mechanisms discussed above.

Mercado [1966] obtained full-aquifer dispersivities of 9 and 15 cm from analysis of the withdrawal-phase concentration histories for two single-well tests (with corresponding average radial front positions in the aquifer at the end of the injection phase estimated to be 6.4 and 16.7 m, respectively) in a sandstone aquifer. The dispersivities from analysis of breakthrough curves at observation wells during the injection phase were somewhat larger (in the range 0.5–1.5 m) and trended toward larger values with increasing radial distances. The larger values of dispersivity from the breakthrough curves at the observation wells were, as pointed out by Mercado, the result of spreading due to stratified flow. *Percious* [1969] determined full-aquifer dispersivities in the range of 8–25 cm from the analysis of the withdrawal-phase concentration histories for the injection-withdrawal well for six single-well tests in an interstratified silt, sand, and gravel deposit. The dispersivities

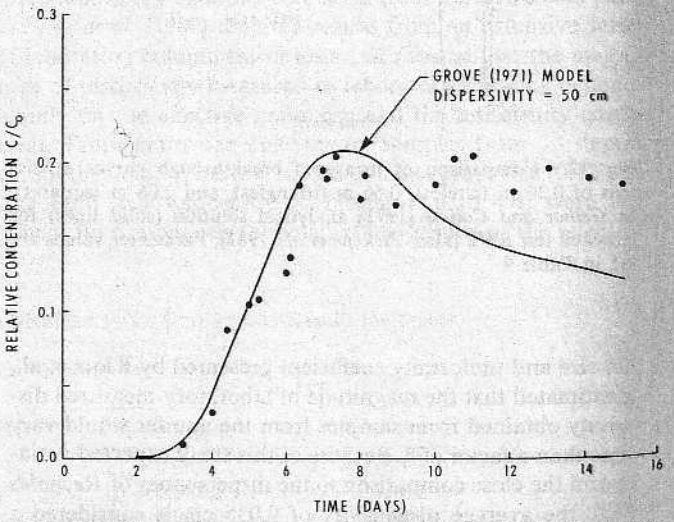

Fig. 14. Comparison of measured (circles) breakthrough curve for withdrawal well with the *Grove* [1971] model (solid line) for the two-well test.

TABLE 10. Relative Hydraulic Conductivity Distribution From the Two-Well Tracer Test

		From Multilevel Sampling Device Results			
		4 m From Injection Well		7 m From Injection Well	
Depth, m	Layer Thickness b_i, m	Time to Reach Peak Concentration, days	Relative Hydraulic Conductivity K_R	Time to Reach Peak Concentration, days	Relative Hydraulic Conductivity K_R
1.37					
2.13	0.44	4.25	0.755	10.42	0.528
2.74	0.53	6.54	0.490	8.75	0.629
3.19	0.45	6.92	0.464	12.67	0.434
3.64	0.45	6.50	0.494	12.42	0.443
4.08	0.45	6.58	0.487	12.42	0.443
4.53	0.45	7.21	0.445	12.42	0.443
4.98	0.45	6.04	0.531	11.25	0.489
5.43	0.45	5.00	0.642	10.00	0.550
5.87	0.45	5.00	0.642	8.38	0.657
6.32	0.45	3.96	0.811	7.46	0.737
6.77	0.45	3.79	0.846	6.46	0.852
7.21	0.45	3.21	1.000	6.38	0.863
7.66	0.45	3.42	0.939	5.50	1.000
8.11	0.45	3.75	0.856	5.50	1.000
8.56	0.45	3.58	0.895	5.83	0.943
9.00	0.45	4.13	0.778	6.25	0.880
9.45	0.53	5.17	0.621	7.21	0.763
10.05	0.40	16.04	0.200	14.04	0.392
10.82					

showed a slight trend to larger values corresponding to the tests with larger average radial front positions in the aquifer at the end of the injection phase (average radial front positions ranged from 1.8 to 5.1 m). Using the same field site as *Percious* [1969], *Wilson* [1971] obtained a dispersivity of 55 cm for an observation well screened over a vertical distance that was 20% of the screened interval of the injection-withdrawal well. This dispersivity was about a factor of 2 larger than the full-aquifer dispersivities obtained from the analysis of the withdrawal-phase concentration histories for the injection-withdrawal well for three tests (dispersivities ranged from 25 cm to 33 cm and the average radial front positions were about 3.4 m).

In general, the full-aquifer dispersivity values obtained by *Percious* [1969] and *Wilson* [1971] from the withdrawal-phase concentration histories are larger than those obtained from this study. This likely reflects the much more heterogeneous nature of the interstratified silt, sand, and gravel deposit in which they conducted their tracer tests. The similarity in full-aquifer dispersivities of *Mercado* [1966] and the present study may suggest that the two aquifers exhibit a similar degree of heterogeneity. In an ideally homogeneous aquifer, the full-aquifer dispersivity from a single-well test would likely approach a laboratory-measured value. For example, the laboratory studies of radial dispersion in homogeneous sand tanks by *Hoopes and Harleman* [1967*a*] and *Hartel* [1972] yielded dispersivities ranging from 0.14 to 0.16 cm and 0.25 to 0.305 cm, respectively.

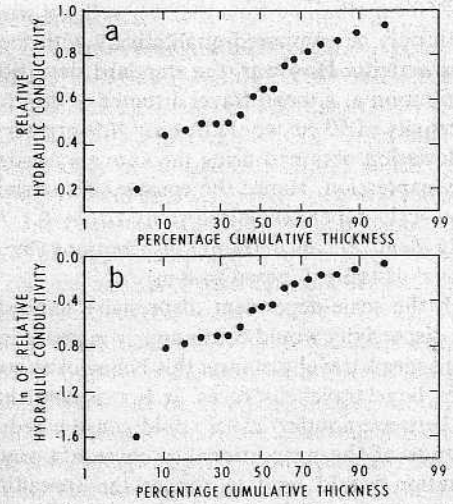

Fig. 15. Plots of (*a*) relative hydraulic conductivity and (*b*) natural logarithm of relative hydraulic conductivity versus percentage cumulative thickness of aquifer for multilevel sampling device results 4 m from injection well of the two-well test.

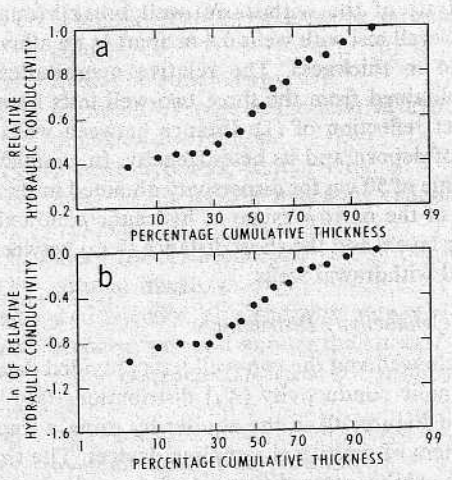

Fig. 16. Plots of (*a*) relative hydraulic conductivity and (*b*) natural logarithm of relative hydraulic conductivity versus percentage cumulative thickness of aquifer for multilevel sampling device results 7 m from injection well of the two-well test.

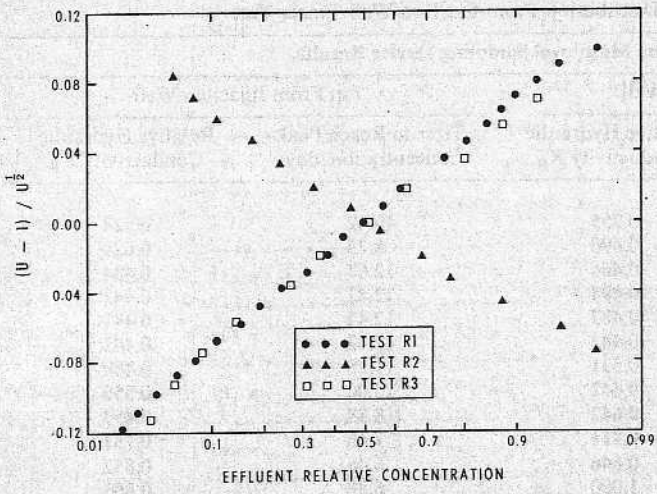

Fig. 17. Plot of $(U-1)/U^{1/2}$ versus effluent relative concentration for the laboratory column tracer tests.

Dispersivities From Two-Well Tests

Analysis of the withdrawal-well breakthrough curve from the two-well test using the *Grove* [1971] model yielded a longitudinal dispersivity of 50 cm for the full aquifer. This dispersivity includes the effect of mixing in the well of water of differing tracer concentrations from the various levels within the aquifer. The full-aquifer dispersivity from a two-well test exhibits a scale effect being dependent on the aquifer characteristics (hydraulic conductivity distribution) and the distance between the injection and withdrawal wells.

Kaufman et al. [1961] presented a withdrawal-well breakthrough curve for a two-well test with wells 30.5 m apart in a consolidated sand and gravel deposit of 1.34 m thickness. Assuming a porosity of 0.30, the breakthrough curve can be analyzed using the *Grove* [1971] model to yield a dispersivity of 2 m. *Wilson* [1971] presented a withdrawal-well breakthrough curve for a two-well test in an interstratified sand, silt, and gravel deposit with the two wells located 79.2 m part. The breakthrough curve could not be fitted very closely with the *Grove* [1971] model, but a rough fit of the early time data (corresponding to $C/C_o < 0.1$) can be obtained using a dispersivity of 100 m with a porosity of 0.35 and an aquifer thickness of 15.2 m. *Robson* [1974] obtained a dispersivity of 15.2 m from analysis of the withdrawal-well breakthrough curve from a two-well test with wells 6.4 m apart in an alluvial aquifer of 27.4 m thickness. The relative magnitudes of dispersivity obtained from the three two-well tests noted above are a direct reflection of (1) distance between wells and (2) thickness of deposit and its heterogeneity. In comparison, the smaller value of 50 cm for dispersivity obtained in this study is indicative of the narrow range of hydraulic conductivities of the aquifer layers and the short distance (8 m) between the injection and withdrawal wells.

Hydraulic Conductivity Distributions

The single-well and the two-well tests provided detailed relative hydraulic conductivity (K_R) distributions (see Tables 6 and 10 and Figure 10) in the aquifer by using a tracer monitoring system of multilevel sampling devices. The single-well test results exhibit some differences in magnitude at specific depths as compared to the two-well test, but the same general trend of relative hydraulic conductivity throughout the aquifer depth is shown by both tracer tests. The similarity in the relative hydraulic conductivity distributions obtained from the two-well test, for multilevel sampling devices at 4 and 7 m from the injection well, provides direct evidence of the continuity of the layering within the aquifer over distances of at least 7 m. Straight-line fits of the plots of K_R and ln K_R versus percent cumulative aquifer thickness (Figures 11, 15, and 16) would illustrate that the hydraulic conductivity distributions obtained from the tracer tests follow a normal or log normal distribution equally well. The observation that hydraulic conductivities of a stratified sandy deposit may fit either a normal or a log normal distribution has also been noted by *Smith* [1980].

Relative hydraulic conductivity distributions can also be evaluated by other methods. For example, hydraulic conductivities were obtained from the grain size analyses of samples from various aquifer depths using the Hazen formula. These values followed a relative hydraulic conductivity trend similar to those obtained from the tracer tests. The relative hydraulic conductivity results obtained from groundwater velocity profiling of the aquifer under natural flow conditions using the borehole dilution method also exhibited a similar trend [*Pickens et al.*, 1980].

Scale-Dependent Full-Aquifer Dispersivity Expressions

The scale-dependent dispersivity expressions for the three stratification types are summarized in Table 8. The longitudinal dispersivity value is a linear function of mean travel distance with proportionality constants ranging from 0.041 to 0.256. This range in magnitude results mainly from differences in the relative hydraulic conductivity distributions interpreted from monitoring tracer movement in the field tracer tests. The average of all proportionality constants is 0.1.

The importance of allowing dispersivity to be a function of mean travel distance lies in the fact that the expression is valid for various distance and time scales. In contrast, the dispersivity of 50 cm obtained from the two-well test is only valid at the spatial scale corresponding to the distance between the well pair (i.e., 8 m). Dispersivity values calculated from the above expression increase linearly from 0 to 80 cm for a mean travel distance increasing from 0 to 8 m. The constant dispersivity of 50 cm obtained from the two-well test with wells 8 m apart can only be compared qualitatively with the linearly varying dispersivity. However, the standard deviation of the tracer distribution at a mean travel distance of 8 m for a constant dispersivity of 50 cm would be only 10% greater than the standard deviation obtained using the above scale-dependent dispersivity expression. Hence the constant dispersivity of 50 cm and the scale-dependent dispersivity ($\alpha_L = 0.1\ L$) would yield nearly identical concentration distributions (but only for a mean travel distance L equal to 8 m).

Although the scale-dependent dispersivity expressions indicate that dispersivity would continuously increase in a linear fashion with mean travel distance, this behavior is considered unlikely for large travel distances. It is expected that tracer migration between aquifer layers could cause a reduction in the magnitude of the proportionality constants, since transverse migration would tend to reduce the spreading effect caused by the stratification. Hydraulic conductivity variations (both longitudinal and lateral) over scales larger than those investigated in the present study would also tend to reduce the spreading caused by stratification. Consequently, it is ex-

pected that dispersivity would approach a maximum or asymptotic value.

Although the early-time scale-dependent dispersivity functions developed in this paper are of a linear type, it is likely that other types of dispersivity functions are possible, whether derived from a theoretical basis or empirically from field tracer tests. Examples of the incorporation of various types of scale-dependent dispersivity functions in a finite element solute transport model and an evaluation of the importance of early-time scale dependence are presented by *Pickens and Grisak* [1981].

CONCLUSIONS

1. The concentration profile within an aquifer or the breakthrough curve at a sampling position are strongly dependent on the type of monitoring system (i.e., groundwater sampling scale). The monitoring system (e.g., multilevel point-sampling devices, piezometers, wells) can result in some apparent spreading. This spreading effect can result in larger estimates of dispersivity.

2. The mean longitudinal dispersivity obtained from analysis of transport at the scale of individual levels in the aquifer for the single-well tests is 0.7 cm. Although the aquifer is known to exhibit laminations of the order of 0.1–0.5 cm, there was no evidence of scale dependence with different travel distances, possibly because a constant or 'asymptotic' dispersivity had been reached at a travel distance closer than the nearest sampling point (i.e., 0.36 m).

3. The full-aquifer dispersivity obtained from analysis of the withdrawal-phase concentration history for the injection-withdrawal well of a single-well test is dependent largely on the effect and extent of transverse migration between layers in response to hydraulic and concentration gradients. Dispersivities of 3 and 9 cm were obtained for tracer tests with average radial front positions of 313 and 499 cm, respectively, at the end of the injection phase. The full-aquifer dispersivity exhibits a scale effect with the value obtained, from the two tests, showing an increase proportional to approximately the square of the average radial front position. The scale-dependent nature of the full-aquifer dispersivity is also evident by comparison to the relatively constant value of 0.7 cm obtained for the individual levels.

4. The full-aquifer longitudinal dispersivity obtained from analysis of the withdrawal-well breakthrough curve of a two-well test is also scale dependent. The dispersivity (50 cm) obtained in this test is representative for describing transport in the aquifer only for situations with full-aquifer groundwater sampling instrumentation (fully penetrating wells) and with the same distance between input and sampling locations (8 m). The full-aquifer dispersivity from a two-well test is dependent on the aquifer hydraulic conductivity distribution and the distance between wells.

5. The average dispersivity value of 0.035 cm, obtained from three laboratory tracer tests with a repacked column of sand, is considered to be a representative laboratory-scale value for sand from the field site. A scale effect is observed between the laboratory dispersivity (0.035 cm) and the dispersivity obtained for individual levels within the aquifer (0.7 cm). This scale effect is the result of (1) greater nonhomogeneity of the aquifer (e.g., laminations) and (2) the averaging caused by the groundwater sampling system.

6. Theoretical scale-dependent dispersivity expressions were developed for normal, log normal, and arbitrary stratification types with input and sampling at the scale of the full aquifer thickness. These expressions relate the magnitude of longitudinal dispersivity to the statistical properties of the stratified medium and the mean travel distance of the solute. By monitoring tracer movement at various levels within the aquifer, detailed relative hydraulic conductivity distributions (vertically) were obtained. For simulating solute transport at the scale of the full aquifer thickness, the following scale-dependent dispersivity expression is representative for the study site aquifer: $\alpha_L = 0.1\ L$, where α_L is the longitudinal dispersivity and L is the mean travel distance. The effect of transverse migration between aquifer layers would become more significant with increasing travel distance, resulting in a reduction in the rate of increase of dispersivity with mean travel distance. The magnitude of the dispersivity is unlikely to increase continually but instead will likely approach a maximum or asymptotic value after some characteristic mean travel distance.

7. The above conclusions have documented the importance of groundwater sampling scale in the interpretation of tracer test results to obtain values for dispersivity. The values of dispersivity or the dispersivity expression that one would choose for use with a predictive model must be consistent with the sampling scale.

NOTATION

A_i quantity equal to $(Q/b)_i/2\pi\theta$, L^2T^{-1}.
b aquifer thickness, L.
b_i thickness of layer i, L.
C concentration in solution, ML^{-3}.
C_0 input concentration, ML^{-3}.
C/C_0 relative concentration.
d distance between withdrawal and injection wells, L.
D hydrodynamic dispersion coefficient, L^2T^{-1}.
D_0 molecular diffusion coefficient in a free-water system, L^2T^{-1}.
D^* molecular diffusion coefficient in saturated porous media, L^2T^{-1}.
h hydraulic head, L.
i subscript denoting a level or layer within the aquifer.
K hydraulic conductivity, LT^{-1}.
K_H harmonic average of the relative hydraulic conductivity distribution.
K_R relative hydraulic conductivity.
$\bar{K}$ mean of the relative hydraulic conductivity distribution.
L mean travel distance, L.
L^* column length, L.
Q well injection or withdrawal rate, L^3T^{-1}.
Q/b recharge per unit aquifer thickness, L_2T^{-1}.
r radial distance coordinate (from injection well), L.
r_w well radius, L.
$\bar{r}$ average radial front position, L.
R average radial front position in the aquifer at the end of the injection phase, L.
S^2 variance of the residence-time distribution.
t time, T.

t_m transit time for plug flow between the two wells of a two-well withdrawal-injection flow field, T.
$t_{0.5}$ time to reach a relative concentration of 0.5, T.
U effluent pore volumes.
U_I total injected volume, L^3.
U_P withdrawal volume at various times during the withdrawal phase, L^3.
V average interstitial pore water velocity, LT^{-1}.
x direction (spatial coordinate), L.
$\bar{x}$ mean travel distance, L.
x Cartesian coordinate direction, L.
α dispersivity, L.
α_L longitudinal dispersivity, L.
α_T transverse dispersivity, L.
$\gamma = (U - 1)/U^{1/2}$.
$\gamma_{0.16}$, $\gamma_{0.84}$ value of γ at relative concentrations of 0.16 and 0.84, respectively.
$\Delta(U_P/U_I)$ dimensionless withdrawal volume increment between the intercepts of the tangent line at $0.5C_0$ with the $C/C_0 = 0.0$ and 1.0 lines.
Δt time increment between the intercepts of the tangent line at $0.5C_0$ with $C/C_0 = 0.0$ and 1.0 lines, T.
θ porosity.
σ standard deviation of tracer distribution, L.
σ^2 variance of tracer distribution, L^2.
σ_K standard deviation of relative hydraulic conductivity distribution.
σ_1 standard deviation of the log normal hydraulic conductivity distribution.
τ dimensionless time, equal to $2Qt/(\pi b\theta d^2)$.

Acknowledgments. Financial and technical support has been provided by Atomic Energy of Canada Limited (Chalk River Nuclear Laboratories) and Environment Canada during these investigations. The authors appreciate the technical assistance of K. J. Inch, the guidance in the use of hydrologic tracers by W. F. Merritt, and the detailed comments on early drafts of the manuscript by J. A. Cherry.

REFERENCES

Bear, J., On the tensor form of dispersion in porous media, *J. Geophys. Res., 66*(4), 1185–1197, 1961*a*.
Bear, J., Some experiments in dispersion, *J. Geophys. Res., 66*(8), 2455–2467, 1961*b*.
Brenner, H., The diffusion model of longitudinal mixing in beds of finite length: Numerical values, *Chem. Eng. Sci., 17,* 229–243, 1962.
Brigham, W. E., Mixing equations in short laboratory columns, *Soc. Pet. Eng. J., 14,* 91–99, 1974.
Chapman, B. M., Dispersion of soluble pollutants in nonuniform rivers, I, Theory, *J. Hydrol., 40*(1/2), 139–152, 1979.
Cherry, J. A., R. E. Jackson, D. C. McNaughton, J. F. Pickens, and H. Woldetensae, Physical hydrogeology of the lower Perch Lake basin, Hydrological Studies on a Small Basin on the Canadian Shield, *Rep. AECL-5041,* vol. 2, edited by P. J. Barry, pp. 625–680, At. Energy of Can., Ltd., Chalk River Nuclear Laboratories, 1975.
Cole, J. A., Some interpretations of dispersion measurements in aquifers, in *Groundwater Pollution in Europe,* edited by J. A. Cole, pp. 86–95, Water Research Association, Reading, England, 1972.
DaCosta, J. A., and R. R. Bennett, The pattern of flow in the vicinity of a recharging and discharging pair of wells in an aquifer having areal parallel flow, *Int. Assoc. Sci. Hydrol. Publ., 52,* 524–536, 1960.
Day, P. R., Dispersion of a moving salt-water boundary advancing through saturated sand, *Eos Trans. AGU, 37*(5), 595–601, 1956.
Day, T. J., Longitudinal dispersion in natural channels, *Water Resour. Res., 11*(6), 909–918, 1975.
DeWiest, R. J. M., *Geohydrology,* 366 pp., John Wiley, 1965.
Einstein, A., Uber die von der molekularkinetischen Theorie der Warme geforderte Bewegung von in Ruhenden Flussigkeiten suspendierten Teinchen, *Ann. Phys., 17,* 549–560, 1905.
Fried, J. J., Miscible pollution of ground water: A study of methodology, in *Proceedings of the International Symposium on Modelling Techniques in Water Resources Systems,* vol. 2, edited by A. K. Biswas, pp. 362–371, Environment Canada, Ottawa, Ont., 1972.
Fried, J. J., *Groundwater Pollution,* 330 pp., Elsevier, New York, 1975.
Fried, J. J., P. C. Leveque, D. Poitrinal, and J. Severac, Local studies of miscible pollutions of groundwater: The single-well pulse technique, in *Groundwater Pollution in Europe,* edited by J. A. Cole, pp. 388–408, Water Research Association, Reading, England, 1972.
Gelhar, L. W., and M. A. Collins, General analysis of longitudinal dispersion in nonuniform flow, *Water Resour. Res., 7*(6), 1511–1521, 1971.
Gelhar, L. W., A. L. Gutjahr, and R. L. Naff, Stochastic analysis of macrodispersion in a stratified aquifer, *Water Resour. Res., 15*(6), 1387–1397, 1979.
Godfrey, R. G., and B. J. Frederick, Stream dispersion at selected sites, *U.S. Geol. Surv. Prof. Pap., 433-K,* 1–38, 1970.
Grisak, G. E., R. E. Jackson, and J. F. Pickens, Monitoring groundwater quality: The technical difficulties, in *Establishment of Water Quality Monitoring Programs, Proceedings of the American Water Resources Association Symposium, 12–14 June 1978, San Francisco,* edited by L. G. Everett and K. D. Schmidt, pp. 210–232, Minneapolis, Minn., 1979.
Grove, D. B., U.S. Geological Survey Tracer Study, Amargosa Desert, Nye County, Nevada, II, An analysis of the flow field of a discharging-recharging pair of wells, *U.S. Geol. Surv. Rep., USGS-474-99,* 56 pp., 1971.
Grove, D. B., and W. A. Beetem, Porosity and dispersion constant calculations for a fractured carbonate aquifer using the two-well tracer method, *Water Resour. Res., 7*(1), 128–134, 1971.
Grove, D. B., W. A. Beetem, and F. B. Sower, Fluid travel time between a recharging and discharging well pair in an aquifer having a uniform regional flow field, *Water Resour. Res., 6*(5), 1404–1410, 1970.
Hartel, C. J., Dispersion in non-uniform porous media, Report to fulfill the requirements of CE 700, Special Problems, Civ. Eng. Dep., Univ. of Mass., Amherst, Dec., 1972.
Hiby, J. W., Longitudinal and transverse mixing during single-phase flow through granular beds, in *Proceedings of Symposium on Interaction Between Fluids and Particles,* pp. 312–325, Institute of Chemical Engineering, London, 1962.
Hoopes, J. A., and D. R. F. Harleman, Dispersion in radial flow from a recharge well, *J. Geophys. Res., 72*(14), 3595–3607, 1967*a*.
Hoopes, J. A., and D. R. F. Harleman, Wastewater recharge and dispersion in porous media, *J. Hydraul. Div. Am. Soc. Civ. Eng., 93*(HY5), 51–71, 1967*b*.
Jackson, R. E., and K. J. Inch, Hydrogeochemical processes affecting the migration of radionuclides in a fluvial sand aquifer at the Chalk River Nuclear Laboratories, *Sci. Ser. 104,* 58 pp., Natl. Hydrol. Res. Inst., Inland Waters Directorate, Environ. Can. Ottawa, Ont. 1980.
James, R. V., and J. Rubin, Accounting for apparatus-induced dispersion in analyses of miscible displacement experiments, *Water Resour. Res., 8*(3), 717–721, 1972.
Kaufman, W. J., B. B. Ewing, J. V. Kerrigan, and Y. Inoue, Disposal of radioactive wastes into deep geologic formation, *J. Water Pollut. Control Fed., 33*(1), 73–84, 1961.
Klotz, D., K.-P. Seiler, H. Moser, and F. Neumaier, Dispersivity and velocity relationship from laboratory and field experiments, *J. Hydrol., 45*(1/2), 169–184, 1980.
Konikow, L. F., Modeling solute transport in ground water, in *Environmental Sensing and Assessment, Proceeding of International Conference, Las Vegas, Nevada,* article 20-3, 6 pp., Institute for Electrical and Electronics Engineers, Piscataway, N. J., 1976.
Konikow, L. F., and J. D. Bredehoeft, Modeling flow and chemical quality changes in an irrigated stream-aquifer system, *Water Resour. Res., 10*(3), 546–562, 1974.
Kreft, A., A. Lenda, B. Turek, A. Zuber, and K. Czauderna, Determination of effective porosities by the two-well pulse method, in *Isotope Techniques in Groundwater Hydrology,* vol. 2, pp. 295–312, International Atomic Energy Agency, Vienna, 1974.
Kruseman, G. P., and N. A. de Ridder, Analysis and evaluation of pumping test data, *Bull. II,* 200 pp., Int. Inst. for Land Reclamation and Improvement, Wageningen, Netherlands, 1970.
Lau, L. K., W. J. Kaufman, G. T. Orlob, and D. K. Todd, Studies of flow dispersion in porous media, *Progr. Rep. 4,* 67 pp., Canal Seepage Res., Univ. of Calif., Berkeley, 1958.

Lau, L. K., W. J. Kaufman, and D. K. Todd, Dispersion of a water tracer in radial laminar flow through homogeneous porous media, *Progr. Rep. 5*, 78 pp., Canal Seepage Res., Univ. of Calif., Berkeley, 1959.

Lee, D. R., J. A. Cherry, and J. F. Pickens, Groundwater transport of a salt tracer through a sandy lakebed, *Limnol. Oceanogr., 25*(1), 45–61, 1980.

Lerman, A., *Geochemical Processes: Water and Sediment Environments*, 481 pp., John Wiley, New York, 1979.

Mansell, R. S., and A. Elseftawy, Measuring chloride in effluent flowing from a soil column, *Soil Sci. Soc. Am. Proc., 36*, 378–380, 1972.

Matheron, G., and D. de Marsily, Is transport in porous media always diffusive? A counter example, *Water Resour. Res., 16*(5), 901–917, 1980.

Mercado, A., Recharge and mixing tests at Yavne 20 well field, *Underground Water Storage Study Tech. Rep. 12, Publ. 611*, 62 pp., TAHAL-Water Planning for Israel Ltd., Tel Aviv, 1966.

Mercado, A., The spreading pattern of injected water in a permeability stratified aquifer, *Int. Assoc. Sci. Hydrol. Publ., 72*, 23–36, 1967.

Merritt, W. F., J. F. Pickens, and G. B. Allison, Study of transport in unsaturated sands using radioactive tracers, Hydrological and Geochemical Studies in the Perch Lake Basin, A Second Report of Progress, *Publ. AECL-6404*, edited by P. J. Barry, pp. 155–164, At. Energy of Can. Ltd., Chalk River Nuclear Laboratories, 1979.

Oakes, D. B., and D. J. Edworthy, Field measurements of dispersion coefficients in the United Kingdom, in *Groundwater Quality, Measurement, Prediction and Protection*, pp. 327–340, Water Research Centre, Reading, England, 1977.

Parsons, P. J., Movement of radioactive waste through soil, 1, Soil and ground-water investigations in lower Perch Lake Basin, *Publ. AECL-1038*, 51 pp. At. Energy of Can. Ltd., Chalk River Nuclear Laboratories, 1960.

Peaudecerf, P., and J. P. Sauty, Application of a mathematical model to the characterization of dispersion effects of groundwater quality, *Progr. Water Tech., 10*(5/6), 443–454, 1978.

Percious, D. J., Aquifer dispersivity by recharge-discharge of a fluorescent dye tracer through a single well, M.Sc. thesis, 80 pp., Dep. of Hydrol. and Water Resour., Univ. of Ariz., Tucson, 1969.

Perkins, T. K., and O. C. Johnston, A review of diffusion and dispersion in porous media, *Soc. Pet. Eng. J., 19*, 70–84, 1963.

Pickens, J. F., The effect of aquifer stratification on the determination of dispersivity, *Geol. Soc. Am. Abstr. Programs*, 472, 1978.

Pickens, J. F., and G. E. Grisak, Reply to discussion by J. A. Vonhof et al. of 'A multilevel device for ground-water sampling and piezometric monitoring,' *Ground Water, 17*(4), 393–397, 1979.

Pickens, J. F., and G. E. Grisak, Modeling of scale-dependent dispersion in hydrogeologic systems, submitted to *Water Resour. Res.*, 1981.

Pickens, J. F., J. A. Cherry, R. W. Gillham, and W. F. Merritt, Field studies of dispersion in a shallow sandy aquifer, Proceedings of Invitational Well Testing Symposium, 19–21 October 1977, *Rep. LB7-7027*, pp. 55–62, Lawrence Berkeley Lab., Berkeley, Calif., 1978*a*.

Pickens, J. F., J. A. Cherry, G. E. Grisak, W. F. Merritt, and B. A. Risto, A multilevel device for ground-water sampling and piezometric monitoring, *Ground Water, 16*(5), 322–327, 1978*b*.

Pickens, J. F., W. F. Merritt, and J. A. Cherry, Field determination of the physical contaminant transport parameters in a sandy aquifer, in *Nuclear Techniques in Water Pollution Studies, Proceedings of Advisory Group Meeting, 6–9 December 1976, Cracow, Poland*, pp. 239–265, International Atomic Energy Agency, Vienna, 1980.

Pickens, J. F., R. E. Jackson, K. J. Inch, and W. F. Merritt, Measurement of distribution coefficients using a radial injection dual-tracer test, *Water Resour. Res., 17*(6), 529–544, 1981.

Pinder, G. F., A Galerkin-finite element simulation of groundwater contamination on Long Island, New York, *Water Resour. Res., 9*(6), 1657–1669, 1973.

Reynolds, W. D., Column studies of strontium and cesium transport through a granular geologic porous medium, M.Sc. thesis, 149 pp., Dep. of Earth Sci., Univ. of Waterloo, Waterloo, Ont., 1978.

Rifai, M. N. E., W. J. Kaufman, and D. K. Todd. Dispersion phenomena in laminar flow through porous media, *Rep. 3, I.E.R. Ser. 90*, 157 pp., Sanit. Eng. Res. Lab., Univ. of Calif., Berkeley, 1956.

Robson, S. G., Feasibility of water-quality modeling illustrated by application at Barstow, California, *Water Resour. Invest. Rep. 46-73*, 66 pp., U. S. Geol. Surv., Menlo Park, Calif., 1974.

Robson, S. G., Application of digital profile modeling techniques to ground-water solute transport at Barstow, California, *U.S. Geol. Surv. Water Supply Pap., 2050*, 28 pp., 1978.

Rousselot, D., Aeroport de Lyon-Satolas, Etude hydrodynamique de couloir fluvioglaciaire de Meyzieux en vue de la protection de la qualite des ressources en eau: Simulation des transferts, *IAHS Publ., 123*, 389–407, 1977.

Sauty, J. P., Identification des parametres du transport hydrodispersif dans les aquiferes par interpretation de tracages en ecoulement cylindrique convergent ou divergent, *J. Hydrol., 39*(3/4), 69–103, 1978.

Sauty, J. P., A. C. Gringarten, and P. A. Landel, The effect of thermal dispersion on injection of hot water in aquifers, Proceedings of Second Invitational Well Testing Symposium, pp. 122–131, Lawrence Berkeley Lab., Berkeley, Calif., 1979.

Scheidegger, A. E., Statistical hydrodynamics in porous media, *J. Appl. Phys., 25*(8), 994–1001, 1954.

Schwartz, C. E., and J. M. Smith, Flow distribution in packed beds, *Ind. Eng. Chem., 45*(6), 1209–1218, 1953.

Schwartz, F. W., Macroscopic dispersion in porous media: The controlling factors, *Water Resour. Res., 13*(4), 743–752, 1977.

Smith, L., Spatial variability of flow parameters in a stratified sand, *Int. J. Math. Geol., 13*(1), 1–21, 1980.

Smith, L., and F. W. Schwartz, Mass transport, 1, A stochastic analysis of macroscopic dispersion, *Water Resour. Res., 16*(2), 303–313, 1980.

Sudicky, E. A., and J. A. Cherry, Field observations of tracer dispersion under natural flow conditions in an unconfined sandy aquifer, *Water Pollut. Res. Can., 14*, 1–17, 1979.

Theis, C. V., Notes on dispersion in fluid flow by geologic features, Proceedings of Conference on Ground Disposal of Radioactive Wastes, Chalk River, Ont., Canada, *Rep. TID-7628*, edited by J. M. Morgan, D. K. Kamison, and J. D. Stevenson, pp. 166–178, U.S. At. Energy Comm., Washington, D. C., 1962.

Theis, C. V., Hydrologic phenomena affecting the use of tracers in timing ground water flow, in *Radioisotopes in Hydrology*, pp. 193–206, International Atomic Energy Agency, Vienna, 1963.

Warren, J. E., and J. J. Cosgrove, Prediction of waterflood behaviour in a stratified system, *Soc. Pet. Eng. J., 4*, 149–157, 1964.

Warren, J. E., and F. F. Skiba, Macroscopic dispersion, *Soc. Pet. Eng. J., 4*, 215–230, 1964.

Webster, D. S., J. F. Proctor, and I. W. Marine, Two-well tracer test in fractured crystalline rock, *U.S. Geol. Surv. Water Supply Pap., 1544-I*, 22 pp., 1970.

Wilson, J. L., and P. J. Miller, Two dimensional plume in uniform, ground-water flow, *J. Hydraul. Div. Am. Soc. Civ. Eng., 104*(HY4), 504–514, 1978.

Wilson, L. G., Investigations on the subsurface disposal of waste effluents at inland sites, *Res. Develop. Progr. Rep. 650*, 106 pp., U.S. Dep. of Interior, Washington, D. C., 1971.

Yotsukura, N., H. B. Fischer, and W. W. Sayre, Mixing characteristics of the Missouri River between Sioux City, Iowa, and Plattsmouth, Nebraska, *U.S. Geol. Surv. Water Supply Pap., 1899*, 1–29, 1970.

(Received January 12, 1981;
revised March 22, 1981;
accepted March 25, 1981.)